Uncovering multiple *CP*-nonconserving mechanisms of $(\beta\beta)_{0\nu}$ decay

Amand Faessler,[1] A. Meroni,[2,3] S. T. Petcov,[2,3,4,*] F. Šimkovic,[5,6] and J. Vergados[7]

[1]*Institute of Theoretical Physics, University of Tuebingen, 72076 Tuebingen, Germany*
[2]*SISSA, Via Bonomea 265, 34136 Trieste, Italy*
[3]*Istituto Nazionale di Fisica Nucleare, Sezione di Trieste, Via Valerio 2, 34126 Trieste, Italy*
[4]*IPMU, University of Tokyo, Tokyo, Japan*
[5]*Department of Nuclear Physics and Biophysics, Comenius University, Mlynska dolina F1, SK-842 15 Bratislava, Slovakia*
[6]*Bogoliubov Laboratory of Theoretical Physics, JINR, 141980 Dubna, Moscow region, Russia*
[7]*Theoretical Physics Devision, University of Ioannina, GR-451 10 Ioannina, Greece*

(Received 31 March 2011; published 7 June 2011)

We consider the possibility of several different mechanisms contributing to the $(\beta\beta)_{0\nu}$-decay amplitude in the general case of *CP* nonconservation: light Majorana neutrino exchange, heavy left-handed and heavy right-handed Majorana neutrino exchanges, lepton charge nonconserving couplings in supersymmetry theories with *R*-parity breaking. If the $(\beta\beta)_{0\nu}$ decay is induced by, e.g., two ''noninterfering'' mechanisms (light Majorana neutrino and heavy right-handed Majorana neutrino exchanges), one can determine $|\eta_i|^2$ and $|\eta_j|^2$, η_i and η_j being the two fundamental parameters characterizing these mechanisms, from data on the half-lives of two nuclear isotopes. In the case when two ''interfering'' mechanisms are responsible for the $(\beta\beta)_{0\nu}$ decay, $|\eta_i|^2$ and $|\eta_j|^2$ and the interference term can be uniquely determined, in principle, from data on the half-lives of three nuclei. Given the half-life of one isotope, the ''positivity conditions'' $|\eta_i|^2 \geq 0$ and $|\eta_j|^2 \geq 0$ lead to stringent constraints on the half-lives of the other $(\beta\beta)_{0\nu}$-decaying isotopes. These conditions, as well as the conditions for constructive (destructive) interference are derived and their implications are analyzed in two specific cases. The experimental limits on neutrino masses obtained in the ^3H β-decay experiments can constrain further the multiple mechanisms of $(\beta\beta)_{0\nu}$ decay if one of the mechanisms involved is the light Majorana neutrino exchange. The measurements of the half-lives with rather high precision and the knowledge of the relevant nuclear matrix elements with relatively small uncertainties is crucial for establishing that more than one mechanism are operative in $(\beta\beta)_{0\nu}$ decay. The method considered by us can be generalized to the case of more than two $(\beta\beta)_{0\nu}$-decay mechanisms. It allows us to treat the cases of *CP* conserving and *CP* nonconserving couplings generating the $(\beta\beta)_{0\nu}$ decay in a unique way.

DOI: 10.1103/PhysRevD.83.113003 PACS numbers: 14.60.Lm, 11.30.Fs, 14.60.Pq

I. INTRODUCTION

If neutrinoless double beta ($(\beta\beta)_{0\nu}$) decay will be observed, it will be of fundamental importance to determine the mechanism which induces the decay. We know that neutrinos have mass and mix, and if they are Majorana particles they should trigger the decay at some probability level. The fundamental parameter which controls the $(\beta\beta)_{0\nu}$-decay rate in this case is the effective Majorana mass:

$$\langle m \rangle = \sum_j^{\text{light}} (U_{ej})^2 m_j, \qquad (\text{all } m_j \geq 0), \qquad (1.1)$$

where U is the Pontecorvo, Maki, Nakagawa and Sakata (PMNS) neutrino mixing matrix [1–3] and m_j are the light Majorana neutrino masses, $m_j \lesssim 1$ eV. The $(\beta\beta)_{0\nu}$-decay rate depends on the type of neutrino mass spectrum which can be hierarchical, with partial hierarchy or quasidegenerate (see, e.g., [4]). Using the data on the neutrino oscillation parameters it is possible to show (see, e.g., [5]) that in the case of the normal hierarchical spectrum one has $|\langle m \rangle| \lesssim 0.005$ eV, while if the spectrum is with inverted hierarchy, 0.01 eV $\lesssim |\langle m \rangle| \lesssim 0.05$ eV. A larger value of $|\langle m \rangle|$ is possible if the light neutrino mass spectrum is with partial hierarchy or of a quasidegenerate type. In the latter case $|\langle m \rangle|$ can be close to the existing upper limits.

The most stringent upper limits on $|\langle m \rangle|$ were set by the IGEX [6], CUORICINO [7] and NEMO3 [8] experiments with ^{76}Ge, ^{130}Te and ^{100}Mo, respectively.[1] The IGEX collaboration has obtained for the half-life of ^{76}Ge, $T^{0\nu}_{1/2} > 1.57 \times 10^{25}$ yr (90% confidence level (C.L.)), from which the limit $|\langle m \rangle| < (0.33\text{–}1.35)$ eV was derived [6]. Using the recent more advanced calculations of the corresponding nuclear matrix elements (including the relevant uncertainties) [9] one finds: $|\langle m \rangle| < (0.22\text{–}0.35)$ eV. The

*Also at: Institute of Nuclear Research and Nuclear Energy, Bulgarian Academy of Sciences, 1784 Sofia, Bulgaria

[1]The NEMO3 collaboration has searched for $(\beta\beta)_{0\nu}$ decay of ^{82}Se and other isotopes as well.

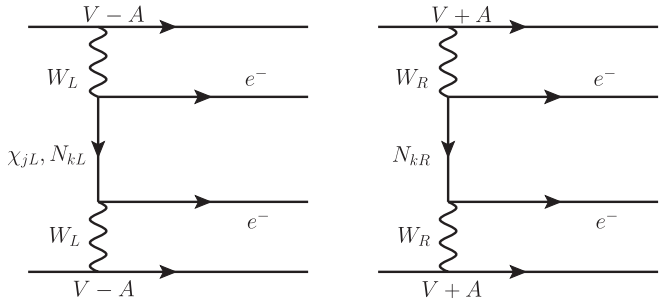

FIG. 1. Feynman diagrams for the $(\beta\beta)_{0\nu}$ decay, generated by the light and heavy LH Majorana neutrino exchange (left panel) and the heavy (RH) Majorana neutrino exchange (right panel).

NEMO3 and CUORICINO experiments, designed to reach a sensitivity to $|\langle m\rangle| \sim (0.2\text{–}0.3)$ eV, set the limits: $|\langle m\rangle| < (0.61\text{–}1.26)$ eV [8] and $|\langle m\rangle| < (0.19\text{–}0.68)$ eV [7] (90% C.L.), where estimated uncertainties in the nuclear matrix element (NME) are accounted for. The two upper limits were derived from the experimental lower limits on the half-lives of ^{100}Mo and ^{130}Te, $T^{0\nu}_{1/2} > 5.8 \times 10^{23}$ yr (90% C.L.) [8] and $T^{0\nu}_{1/2} > 3.0 \times 10^{24}$ yr (90% C.L.) [7]. With the NMEs and their uncertainties calculated in [9], the NEMO3 and CUORICINO upper limits read, respectively: $|\langle m\rangle| < (0.50\text{–}0.96)$ eV and $|\langle m\rangle| < (0.25\text{–}0.43)$ eV. The best lower limit on the half-life of ^{76}Ge, $T^{0\nu}_{1/2} > 1.9 \times 10^{25}$ yr (90% C.L.), was found in the Heidelberg-Moscow ^{76}Ge experiment [10]. It corresponds to the upper limit [9] $|\langle m\rangle| < (0.20\text{–}0.35)$ eV. A positive $(\beta\beta)_{0\nu}$-decay signal at $>3\sigma$, corresponding to $T^{0\nu}_{1/2} = (0.69\text{–}4.18) \times 10^{25}$ yr (99.73% C.L.) and implying $|\langle m\rangle| = (0.1\text{–}0.9)$ eV, is claimed to have been observed in [11], while a later analysis reports evidence for $(\beta\beta)_{0\nu}$ decay at 6σ corresponding to $|\langle m\rangle| = 0.32 \pm 0.03$ eV [12].

Most importantly, a large number of projects aim at a sensitivity to $|\langle m\rangle| \sim (0.01\text{–}0.05)$ eV [13]: CUORE (^{130}Te), GERDA (^{76}Ge), SuperNEMO, EXO (^{136}Xe), MAJORANA (^{76}Ge), MOON (^{100}Mo), COBRA (^{116}Cd), XMASS (^{136}Xe), CANDLES (^{48}Ca), KamLAND-Zen (^{136}Xe), SNO+ (^{150}Nd), etc. These experiments, in particular, will test the positive result claimed in [12]. Let us note that the measurement of $|\langle m\rangle|$ can provide unique information on the absolute scale of neutrino masses, the type of neutrino mass spectrum and the Majorana phases in the PMNS matrix [14].

The light Majorana neutrino exchange can be called the "standard" mechanism of the $(\beta\beta)_{0\nu}$ decay. The observation of $(\beta\beta)_{0\nu}$ decay would imply that the total lepton charge L is not conserved. This would also imply that the massive neutrinos get a Majorana mass [15] and therefore are Majorana particles (see, e.g. [16]). However, the latter does not guarantee that the dominant mechanism inducing the $(\beta\beta)_{0\nu}$ decay is the light Majorana neutrino exchange since the Majorana mass thus generated is exceedingly small. The $(\beta\beta)_{0\nu}$ decay can well be due to the existence of interactions which do not conserve the total lepton charge L, $\Delta L = \pm 2$. A number of such interactions have been proposed in the literature: heavy Majorana neutrinos coupled to the electron in the $V - A$ charged current weak interaction Lagrangian, supersymmetric (SUSY) theories with R-parity breaking terms which do not conserve the total lepton charge L, L-nonconserving couplings in the left-right symmetric theories, etc. At present we do not have evidence for the existence of $\Delta L \neq 0$ terms in the Lagrangian describing the particle interactions. Nevertheless, such terms can exist and they can be operative in the $(\beta\beta)_{0\nu}$ decay. Moreover, it is impossible to exclude the hypothesis that, if observed, the $(\beta\beta)_{0\nu}$ decay is triggered by more than one competing mechanisms.

The possibility of several different mechanisms contributing to the $(\beta\beta)_{0\nu}$-decay amplitude was considered recently in [17] assuming that the corresponding $\Delta L = \pm 2$ couplings are CP conserving. By exploiting the dependence of the nuclear matrix elements on the decaying nucleus, it was shown that, given the experimental observation of the $(\beta\beta)_{0\nu}$ decay of a sufficient number of nuclei, one can determine and/or sufficiently constrain the fundamental parameters associated with the lepton charge nonconserving couplings generating the $(\beta\beta)_{0\nu}$ decay.

The present work is a natural continuation of the study performed in [17]. We consider the possibility of several

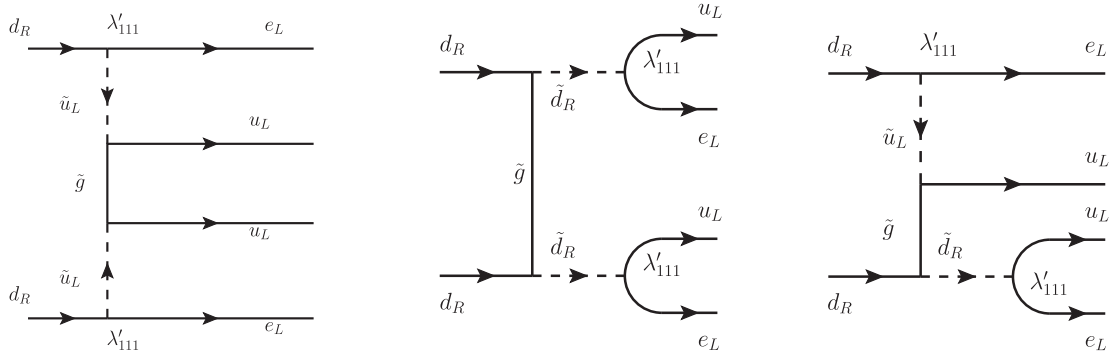

FIG. 2. Feynman diagrams for the $(\beta\beta)_{0\nu}$ decay due to the gluino exchange mechanism.

different mechanisms contributing to the $(\beta\beta)_{0\nu}$-decay amplitude in the general case of *CP* nonconservation: light Majorana neutrino exchange, heavy "left-handed" (LH) and heavy "right-handed" (RH) Majorana neutrino exchanges, lepton charge nonconserving couplings in SUSY theories with *R*-parity breaking. If the $(\beta\beta)_{0\nu}$ decay is induced by, e.g., two "noninterfering" mechanisms (light Majorana neutrino and heavy RH Majorana neutrino exchanges), one can determine the absolute values of the two fundamental parameters, characterising these mechanisms, from data on the half-lives of two nuclear isotopes. In the case when two "interfering" mechanisms are responsible for the $(\beta\beta)_{0\nu}$ decay, the absolute values of the two relevant parameters and the interference term can be uniquely determined from data on the half-lives of three nuclei. In the specific examples considered of two "noninterfering" and two interfering mechanisms, namely, the light Majorana neutrino and the heavy RH Majorana neutrino exchanges, and the light Majorana neutrino and the dominant gluino exchanges, we present illustrative examples of determination of the relevant fundamental parameters and of possible tests of the hypothesis that more than one mechanism is responsible for the $(\beta\beta)_{0\nu}$ decay, using as input hypothetical half-lives of ^{76}Ge, ^{130}Te and ^{100}Mo. The effects of the uncertainties in the values of the NMEs on the results of the indicated analyses are also discussed and illustrated.

The method considered by us can be generalized to the case of more than two $(\beta\beta)_{0\nu}$-decay mechanisms. It also has the advantage that it allows us to treat the cases of *CP* conserving and *CP* nonconserving couplings generating the $(\beta\beta)_{0\nu}$ decay in a unique way.

II. DIFFERENT MECHANISMS OF $(\beta\beta)_{0\nu}$ DECAY

We will consider in the present article the following mechanisms of $(\beta\beta)_{0\nu}$ decay: the exchange of light Majorana neutrinos; the exchange of heavy LH Majorana neutrinos; the exchange of heavy RH Majorana neutrinos; and two mechanisms associated with possible *R*-parity breaking in SUSY theories. Below we discuss briefly the lepton number violating (LNV) parameters and the nuclear matrix elements associated with each of the indicated mechanisms.

Assuming the dominance of a single LNV mechanism characterized by a parameter $\eta_\kappa^{\rm LNV}$, where the index κ denotes the mechanism, the inverse value of the $(\beta\beta)_{0\nu}$-decay half-life for a given isotope (A, Z) can be written as

$$\frac{1}{T^{0\nu}_{1/2}} = |\eta_\kappa^{\rm LNV}|^2 G^{0\nu}(E_0, Z)|M'^{0\nu}_\kappa|^2, \tag{2.1}$$

where $G^{0\nu}(E_0, Z)$ and $M'^{0\nu}_\kappa$ are, respectively, the known phase-space factor (E_0 is the energy release) and the nuclear matrix element of the decay. The latter depends on the mechanism generating the decay and on the nuclear structure of the specific isotopes (A, Z), $(A, Z+1)$ and $(A, Z+2)$ under study.

The phase-space factors $G^{0\nu}(E_0, Z)$, which include the fourth power of the standard value of the axial-coupling constant $g_A = 1.25$, are tabulated in Ref. [18]; for ^{76}Ge, ^{82}Se, ^{100}Mo and ^{130}Te, they are given in Table I. For a given isotope (A, Z), $G^{0\nu}(E_0, Z)$ contains the inverse square of the nuclear radius $R(A)$ of the isotope, $R^{-2}(A)$, compensated by the factor $R(A)$ in $M'^{0\nu}_\kappa$. The assumed value of the nuclear radius is $R(A) = r_0 A^{1/3}$ with $r_0 = 1.1$ fm.

The nuclear matrix element $M'^{0\nu}_\kappa$ is defined as

$$M'^{0\nu}{}_\kappa = \left(\frac{g_A}{1.25}\right)^2 M^{0\nu}_\kappa. \tag{2.2}$$

This definition of $M'^{0\nu}{}_\kappa$ [19] allows us to display the effects of uncertainties in g_A and to use the same phase factor $G^{0\nu}(E_0, Z)$ when calculating the $(\beta\beta)_{0\nu}$-decay rate.

A. Light Majorana neutrino exchange

In the case of the light Majorana neutrino exchange mechanism of $(\beta\beta)_{0\nu}$ decay (see Fig. 1), the LNV parameter is given by:

$$\eta_\nu = \frac{\langle m\rangle}{m_e}, \tag{2.3}$$

where $\langle m\rangle$ is the effective Majorana mass (see, e.g., [16]). Under the assumption of n light massive Majorana neutrinos coupled to the electron in the weak charged lepton current, the effective Majorana mass is given in Eq. (1.1). Thus, $\langle m\rangle$ depends on the elements of first row of the PMNS neutrino mixing matrix, U_{ej}, $j = 1, 2, 3, \ldots$. The PMNS matrix U is not assumed to be *CP* conserving and at least two of the elements U_{ej} contain physical *CP* violating phases [20,21] (see also, e.g., [5]). In the case of 3 light neutrinos and the standard parametrization of U [5], the elements U_{e2} and U_{e3} contain the two physical *CP* violating Majorana phases [20] and U_{e3} contains the Dirac phase as well.

The expression for $\langle m\rangle$, Eq. (1.1), corresponds to the contribution from the standard $(V-A)$ charged current (CC) weak interaction. The nuclear matrix element $M^{0\nu}_\nu$ for different isotopes (A, Z) is given in [18,22] (see also Table I).

B. Heavy Majorana neutrino exchange mechanisms

We assume that the neutrino mass spectrum includes, in addition to the three light Majorana neutrinos, heavy Majorana states N_k with masses M_k much larger than the typical energy scale of the $(\beta\beta)_{0\nu}$ decay, $M_k \gg 100$ MeV; we will consider the case of $M_k \gtrsim 10$ GeV. Such a possibility arises if the weak interaction Lagrangian includes RH sterile neutrino fields which couple to the LH flavor neutrino fields via the neutrino Yukawa coupling and possess a Majorana mass term. The heavy Majorana neutrinos N_k can mediate the $(\beta\beta)_{0\nu}$ decay [23] similar to the light

TABLE I. The phase-space factor $G^{0\nu}(E_0, Z)$ and the nuclear matrix elements $M'^{0\nu}{}_{\nu}$ (light Majorana neutrino exchange mechanism), $M'^{0\nu}{}_{N}$ (heavy Majorana neutrino exchange mechanism), $M'^{0\nu}{}_{\lambda'}$ (mechanism of gluino exchange dominance in SUSY with a trilinear R-parity breaking term) and $M'^{0\nu}{}_{\tilde{q}}$ (squark-neutrino mechanism) for the $(\beta\beta)_{0\nu}$ decays of ^{76}Ge, ^{100}Se, ^{100}Mo and ^{130}Te. The NMEs were obtained within the SRQRPA. See text for details.

Nuclear transition	$G^{0\nu}(E_0, Z)$ [y^{-1}]			$\lvert M'^{0\nu}_{\nu}\rvert$ $g_A =$		$\lvert M'^{0\nu}_{N}\rvert$ $g_A =$		$\lvert M'^{0\nu}_{\lambda'}\rvert$ $g_A =$		$\lvert M'^{0\nu}_{\tilde{q}}\rvert$ $g_A =$	
		NN pot.	m.s.	1.0	1.25	1.0	1.25	1.0	1.25	1.0	1.25
^{76}Ge → ^{76}Se	7.98×10^{-15}	Argonne	intm.	3.85	4.75	172.2	232.8	387.3	587.2	396.1	594.3
			large	4.39	5.44	196.4	264.9	461.1	699.6	476.2	717.8
		CD-Bonn	intm.	4.15	5.11	269.4	351.1	339.7	514.6	408.1	611.7
			large	4.69	5.82	317.3	411.5	392.8	595.6	482.7	727.6
^{82}Se → ^{82}Kr	3.53×10^{-14}	Argonne	intm.	3.59	4.54	164.8	225.7	374.5	574.2	379.3	577.9
			large	4.18	5.29	193.1	262.9	454.9	697.7	465.1	710.2
		CD-Bonn	intm.	3.86	4.88	258.7	340.4	328.7	503.7	390.4	594.5
			large	4.48	5.66	312.4	408.4	388.0	594.4	471.8	719.9
^{100}Mo → ^{100}Ru	5.73×10^{-14}	Argonne	intm.	3.62	4.39	184.9	249.8	412.0	629.4	405.1	612.1
			large	3.91	4.79	191.8	259.8	450.4	690.3	449.0	682.6
		CD-Bonn	intm.	3.96	4.81	298.6	388.4	356.3	543.7	415.9	627.9
			large	4.20	5.15	310.5	404.3	384.4	588.6	454.8	690.5
^{130}Te → ^{130}Xe	5.54×10^{-14}	Argonne	intm.	3.29	4.16	171.6	234.1	385.1	595.2	382.2	588.9
			large	3.34	4.18	176.5	239.7	405.5	626.0	403.1	620.4
		CD-Bonn	intm.	3.64	4.62	276.8	364.3	335.8	518.8	396.8	611.1
			large	3.74	4.70	293.8	384.5	350.1	540.3	416.3	640.7

Majorana neutrinos via the $V - A$ charged current weak interaction. The difference between the two mechanisms is that, unlike the light Majorana neutrino exchange which leads to a long-range internucleon interaction, in the case of $M_k \gtrsim 10$ GeV of interest, the momentum dependence of the heavy Majorana neutrino propagators can be neglected (i.e., the N_k propagators can be contracted to points) and, as a consequence, the corresponding effective nucleon transition operators are local. The LNV parameter in the case when the $(\beta\beta)_{0\nu}$ decay is generated by the $(V - A)$ CC weak interaction due to the exchange of N_k can be written as:

$$\eta_N^L = \sum_k^{\text{heavy}} U_{ek}^2 \frac{m_p}{M_k}, \tag{2.4}$$

where m_p is the proton mass and U_{ek} is the element of the neutrino mixing matrix through which N_k couples to the electron in the weak charged lepton current. We note that $|\eta_N^L|$ is suppressed by both the ratio m_p/M_k and the magnitude of U_{ek} (see, e.g., [24]).

If the weak interaction Lagrangian contains also $(V + A)$ (i.e., right-handed) charged currents coupled to a RH charged weak boson W_R, as, e.g., in the left-right symmetric theories, we can have also a contribution to the $(\beta\beta)_{0\nu}$-decay amplitude generated by the exchange of virtual N_k coupled to the electron in the hypothetical $(V + A)$ CC part of the weak interaction Lagrangian (see Fig. 1) [25]. In this case, the corresponding LNV parameter can be written as:

$$\eta_N^R = \left(\frac{M_W}{M_{WR}}\right)^4 \sum_k^{\text{heavy}} V_{ek}^2 \frac{m_p}{M_k}. \tag{2.5}$$

Here V_{ek} are the elements of a mixing matrix by which N_k couples to the electron in the $(V + A)$ charged lepton current,[2] M_W is the mass of the standard model charged weak boson, $M_W \cong 80$ GeV, and M_{WR} is the mass of W_R. It follows from the existing data that [26] $M_{WR} \gtrsim 2.5$ TeV. Thus, $|\eta_N^R|$ is suppressed by the factor $(M_W/M_{WR})^4$.

If CP invariance does not hold, which we will assume to be the case in what follows, U_{ek} and V_{ek} will contain physical CP violating phases at least for some k and thus the parameters η_N^L and η_N^R will not be real.

As can be shown, the nuclear matrix elements corresponding to the two mechanisms of $(\beta\beta)_{0\nu}$ decay with exchange of heavy Majorana neutrinos N_k, described in the present subsection, are the same and are given in [18]. We will denote them by $M_N^{0\nu}$ (and $M_N'^{0\nu}$).

Finally, it is important to note that the current factor in the $(\beta\beta)_{0\nu}$-decay amplitude describing the two final state electrons, has different forms in the cases of $(\beta\beta)_{0\nu}$ decay mediated by $(V - A)$ and by $(V + A)$ CC weak interactions, namely, $\bar{e}(1 + \gamma_5)e^c \equiv 2\bar{e}_L(e^c)_R$ and $\bar{e}(1 - \gamma_5)e^c \equiv 2\bar{e}_R(e^c)_L$, respectively, where $e^c = C(\bar{e})^T$, C being the charge conjugation matrix (see, e.g., [16]). The difference in the chiral structure of the two currents leads to a specific

[2]We have neglected the contributions to η_N^R, and, more generally, to the $(\beta\beta)_{0\nu}$-decay amplitude due to the possible but small mixing between W and W_R bosons.

phase-space factor of the interference term in the rate of $(\beta\beta)_{0\nu}$ decay, triggered by two mechanisms whose respective contributions to the $(\beta\beta)_{0\nu}$-decay amplitude involve the two different electron current factors. The phase-space factor of the interference term under discussion is significantly smaller than the phase-space factors of the contributions to the $(\beta\beta)_{0\nu}$-decay rate due to each of the two mechanisms, which leads to a relatively strong suppression of the interference term [27] (see further).

C. SUSY models with R-parity nonconservation

The SUSY models with R-parity nonconservation include LNV couplings which can trigger the $(\beta\beta)_{0\nu}$ decay. Let us recall that the R-parity is a multiplicative quantum number defined by $R = (-1)^{2S+3B+L}$, where S, B and L are the spin, the baryon and lepton numbers of a given particle. The ordinary (standard model) particles have $R = +1$, while their superpartners carry $R = -1$. The LNV couplings emerge in this class of SUSY models from the R-parity breaking (R_p) part of the superpotential

$$W_{\not R_p} = \lambda_{ijk} L_i L_j E^c_k + \lambda'_{ijk} L_i Q_j D^c_k + \mu_i L_i H_2, \qquad (2.6)$$

where L, Q stand for lepton and quark $SU(2)_L$ doublet left-handed superfields, while E^c, D^c for lepton and down quark singlet superfields. Here we concentrate only on the trilinear λ'-couplings. The λ'-couplings of the first family of particles and sparticles relevant for $(\beta\beta)_{0\nu}$ decay are given in terms of the fields of the LH electron, electron neutrino ν_{eL}, LH selectron $\tilde{e}_L$ and sneutrino $\tilde{\nu}_{eL}$, LH and RH u- and d-quarks, $u_{L,R}$ and $d_{L,R}$, and LH and RH u- and d-squarks, $\tilde{u}_{L,R}$, $\tilde{d}_{L,R}$, by:

$$\mathcal{L}_{\not R_p} = \lambda'_{111}\Big[(\bar{u}_L \bar{d}_L)\begin{pmatrix} e^c_R \\ -\nu^c_{eR}\end{pmatrix}\tilde{d}_R + (\bar{e}_L \bar{\nu}_{eL}) d_R \begin{pmatrix} \tilde{u}^*_L \\ -\tilde{d}^*_L\end{pmatrix} + (\bar{u}_L \bar{d}_L) d_R \begin{pmatrix} \tilde{e}^*_L \\ -\tilde{\nu}^*_{eL}\end{pmatrix}\Big] + \text{H.c.} \qquad (2.7)$$

At the quark-level there are basically two types of $\not R_p$ SUSY mechanisms of $(\beta\beta)_{0\nu}$ decay: a short-range one with an exchange of heavy Majorana and scalar SUSY particles (gluinos and squarks, and/or neutralinos and selectrons) [28–33], and a long-range mechanism involving the exchange of both heavy squarks and light Majorana neutrinos [34–38]. We will call the latter the ''squark-neutrino'' mechanism.

1. The case of gluino exchange dominance

Assuming the dominance of the gluino exchange in the short-range mechanism (see Fig. 2), one obtains the following expression for the corresponding LNV parameter:

$$\eta_{\lambda'} = \frac{\pi\alpha_s}{6}\frac{\lambda'^2_{111}}{G_F^2 m^4_{\tilde{d}_R}}\frac{m_p}{m_{\tilde{g}}}\Big[1 + \Big(\frac{m_{\tilde{d}_R}}{m_{\tilde{u}_L}}\Big)^2\Big]^2. \qquad (2.8)$$

Here, G_F is the Fermi constant, $\alpha_s = g_3^2/(4\pi)$, g_3 being the $SU(3)_c$ gauge coupling constant. $m_{\tilde{u}_L}$, $m_{\tilde{d}_R}$ and $m_{\tilde{g}}$ are masses of the LH u-squark, RH d-squark and gluino, respectively.

The nuclear matrix element associated with the gluino exchange mechanism, $M^{0\nu}_{\lambda'}$, was calculated in [39,40]. The electron current factor in the term of the $(\beta\beta)_{0\nu}$-decay amplitude corresponding to the gluino exchange mechanism under discussion has the form $\bar{e}(1+\gamma_5)e^c \equiv 2\bar{e}_L(e^c)_R$, i.e., it coincides with that of the light (or heavy LH) Majorana neutrino exchange. Thus, when calculating the $(\beta\beta)_{0\nu}$-decay rate, the interference between the two terms present in the $(\beta\beta)_{0\nu}$-decay amplitude, corresponding to the indicated two mechanisms, has the same phase-space factor as the contributions due to each of the two mechanisms. As a consequence, the interference term will not suffer from phase-space suppression.

2. The squark-neutrino mechanism

In the case of squark-neutrino exchange [38], the $(\beta\beta)_{0\nu}$-decay amplitude does not vanish in the limit of zero Majorana neutrino mass, in contrast to the case of the standard light (LH) Majorana neutrino exchange. This is a consequence of the chiral structure of the corresponding R_p SUSY couplings. The contribution due to the squark-neutrino exchange to the $(\beta\beta)_{0\nu}$-decay amplitude is roughly proportional to the momentum of the virtual neutrino, which is of the order of the Fermi momentum of the nucleons inside of the nucleus, $p_F \approx 100$ MeV. The corresponding LNV parameter is defined as [38]

$$\eta_{\tilde{q}} = \sum_k \frac{\lambda'_{11k}\lambda'_{1k1}}{2\sqrt{2}G_F}\sin 2\theta^d_{(k)}\Big(\frac{1}{m^2_{\tilde{d}_1(k)}} - \frac{1}{m^2_{\tilde{d}_2(k)}}\Big). \qquad (2.9)$$

Here we use the notations $d_{(k)} = d$, s, b and assume that there are 3 light Majorana neutrinos. This LNV parameter vanishes in the absence of $\tilde{d}_{kL} - \tilde{d}_{kR}$-mixing, i.e., when $\theta^d = 0$. The nuclear matrix element for the squark-neutrino mechanism, $M^{0\nu}_{\tilde{q}}$, is given in [38].

III. NUCLEAR STRUCTURE CALCULATIONS

In what follows the $(\beta\beta)_{0\nu}$-decay nuclear matrix elements $M'^{0\nu}_{\nu}$, $M'^{0\nu}_{N}$, $M'^{0\nu}_{\lambda'}$ and $M'^{0\nu}_{\tilde{q}}$ are evaluated for ^{76}Ge, ^{82}Se, ^{100}Mo and ^{130}Te. These nuclei are considered as the most probable candidate sources for the next generation of experiments searching for $(\beta\beta)_{0\nu}$ decay.

We used the Self-consistent Renormalized Quasiparticle Random Phase Approximation (SRQRPA) [41] to calculate the nuclear matrix elements (NMEs) of interest. The SRQRPA takes into account the Pauli exclusion principle and conserves the mean particle number in the correlated ground state.

For each of the four nuclei, two choices of single-particle basis are considered. The intermediate size model

space has 12 levels (oscillator shells $N = 2$–4) for ^{76}Ge and ^{82}Se, 16 levels (oscillator shells $N = 2$–4 plus the $f + h$ orbits from $N = 5$) for ^{100}Mo and 18 levels (oscillator shells $N = 3$, 4 plus $f + h + p$ orbits from $N = 5$) for ^{130}Te. The large size single-particle space contains 21 levels (oscillator shells $N = 0$–5) for ^{76}Ge, ^{82}Se and ^{100}Mo, and 23 levels for ^{130}Te ($N = 1$–5 and i orbits from $N = 6$). In comparison with previous studies [19], we omitted the small space model which is not sufficient to describe realistically the tensor part of the $(\beta\beta)_{0\nu}$-decay nuclear matrix elements.

The single-particle energies were obtained by using a Coulomb–corrected Woods–Saxon potential. Two-body G-matrix elements we derived from the Argonne and the charge dependent Bonn (CD-Bonn) one-boson exchange potential within the Brueckner theory. The schematic pairing interactions have been adjusted to fit the empirical pairing gaps [42]. The particle-particle and particle-hole channels of the G-matrix interaction of the nuclear Hamiltonian H are renormalized by introducing the parameters g_{pp} and g_{ph}, respectively. The calculations have been carried out for $g_{ph} = 1.0$. The particle-particle strength parameter g_{pp} of the SRQRPA is fixed by the data on the two-neutrino double beta decays [19,22]. In the calculation of the $(\beta\beta)_{0\nu}$-decay NMEs, the two-nucleon short-range correlations derived from same potential as residual interactions, namely, from the Argonne or CD-Bonn potentials, were considered [43].

The calculated NMEs $M'^{0\nu}{}_{\nu}$, $M'^{0\nu}{}_{N}$, $M'^{0\nu}{}_{\lambda'}$ and $M'^{0\nu}{}_{\tilde{q}}$ are listed in Table I. We see that a significant source of uncertainty is the value of the axial-vector coupling constant g_A. Further, the NMEs associated with heavy neutrino exchange are also sensitive to the choice of the Nucleon-Nucleon interaction, the CD-Bonn or Argonne potential. These types of realistic Nucleon-Nucleon interaction differ mostly by the description of the short-range interactions.

Finally, we notice that all NMEs given in Table I are real and positive.

IV. ANALYSIS

We illustrate the possibility of getting information about the different LNV parameters when two or more mechanisms are operative in $(\beta\beta)_{0\nu}$ decay, analysing the following two cases. First we consider two competitive "noninterfering" mechanisms of $(\beta\beta)_{0\nu}$ decay: light left-handed Majorana neutrino exchange and heavy right-handed Majorana neutrino exchange. In this case the interference term arising in the $(\beta\beta)_{0\nu}$-decay half-life from the product of the contributions due to the two mechanisms in the $(\beta\beta)_{0\nu}$-decay amplitude, is strongly suppressed [27] as a consequence of the different chiral structure of the final state electron current in the two amplitudes. The latter leads to a different phase-space factor for the interference term, which is typically by a factor of 10 smaller than the standard one (corresponding to the contribution to the $(\beta\beta)_{0\nu}$-decay half-life of each of the two mechanisms). More specifically, the suppression factors for ^{76}Ge, ^{82}Se, ^{100}Mo and ^{130}Te read, respectively [27]: 0.13; 0.08; 0.075 and 0.10. It is particularly small for ^{48}Ca: 0.04. In the analysis which follows we will neglect the contribution of the interference term in the $(\beta\beta)_{0\nu}$-decay half-life. The effect of taking into account the interference term on the results thus obtained, as our numerical calculations have shown, does not exceed approximately 10%.

In the case of the negligible interference term, the inverse value of the $(\beta\beta)_{0\nu}$-decay half-life for a given isotope (A, Z) is given by:

$$\frac{1}{T^{0\nu}_{1/2,i} G^{0\nu}_i(E,Z)} \cong |\eta_\nu|^2 |M'^{0\nu}_{i,\nu}|^2 + |\eta_R|^2 |M'^{0\nu}_{i,N}|^2, \quad (4.1)$$

where the index i denotes the isotope. The values of the phase-space factor $G^{0\nu}_i(E, Z)$ and of the NMEs $M'^{0\nu}{}_{i,\nu}$ and $M'^{0\nu}{}_{i,N}$ for ^{76}Ge, ^{82}Se, ^{100}Mo and ^{130}Te are listed in Table I. The parameters $|\eta_\nu|$ and $|\eta_R|$ are defined in Eqs. (2.3) and (2.5).

In the second illustrative case, we consider $(\beta\beta)_{0\nu}$ decay triggered by two active and interfering mechanisms: the light Majorana neutrino exchange and the gluino exchange. In this case, for a given nucleus, the inverse of the $(\beta\beta)_{0\nu}$-decay half-life is given by:

$$\frac{1}{T^{0\nu}_{1/2,i} G^{0\nu}_i(E,Z)} = |\eta_\nu|^2 |M'^{0\nu}{}_{i,\nu}|^2 + |\eta_{\lambda'}|^2 |M'^{0\nu}{}_{i,\lambda'}|^2 + 2\cos\alpha |M'^{0\nu}{}_{i,\lambda'}||M'^{0\nu}{}_{i,\nu}||\eta_\nu||\eta_{\lambda'}|. \quad (4.2)$$

Here $|\eta_{\lambda'}|$ is the basic parameter of the gluino exchange mechanism defined in Eq. (2.8) and α is the relative phase of $\eta_{\lambda'}$ and η_ν. The values of the NMEs of the mechanisms considered are listed in Table I.

In the illustrative examples of how one can extract information about $|\eta_\nu|$, $|\eta_R|$, etc., we use as input, hypothetical values of the $(\beta\beta)_{0\nu}$-decay half-life of ^{76}Ge satisfying the existing lower limits and the value claimed in Refs. [10,12], as well as the following hypothetical ranges for $T^{0\nu}_{1/2}(^{100}\text{Mo})$ and $T^{0\nu}_{1/2}(^{130}\text{Te})$:

$$\begin{aligned} &T^{0\nu}_{1/2}(^{76}\text{Ge}) \geq 1.9 \times 10^{25}\ \text{y}, \\ &T^{0\nu}_{1/2}(^{76}\text{Ge}) = 2.23^{+0.44}_{-0.31} \times 10^{25}\ \text{y}, \\ &5.8 \times 10^{23}\ \text{y} \leq T^{0\nu}_{1/2}(^{100}\text{Mo}) \leq 5.8 \times 10^{24}\ \text{y}, \\ &3.0 \times 10^{24}\ \text{y} \leq T^{0\nu}_{1/2}(^{130}\text{Te}) \leq 3.0 \times 10^{25}\ \text{y}. \end{aligned} \quad (4.3)$$

Let us note that 5.8×10^{23} y and 3.0×10^{24} y are the existing lower bounds on the half-lives of ^{100}Mo and ^{130}Te [7,8].

In the analysis which follows we will present numerical results first for $g_A = 1.25$ and using the NMEs calculated with the large size single-particle basis ("large basis") and

the CD-Bonn potential. Later results for $g_A = 1.0$, as well as for NMEs calculated with the Argonne potential, will also be reported.

As we will see, in certain cases of at least one more mechanism being operative in $(\beta\beta)_{0\nu}$ decay beyond the light neutrino exchange, one has to take into account the upper limit on the absolute scale of neutrino masses set by the ^3H β-decay experiments [44,45]: $m(\bar{\nu}_e) < 2.3$ eV. In the case of $(\beta\beta)_{0\nu}$ decay, this limit implies a similar limit on the effective Majorana mass [3] $|\langle m\rangle| < 2.3$ eV. The latter translates into the following limit on the conveniently rescaled parameter $|\eta_\nu|^2$:

$$|\eta_\nu|^2 \times 10^{10} < 0.21. \tag{4.4}$$

A more stringent limit on the absolute neutrino mass scale and therefore on $|\langle m\rangle|$ is planned to be obtained in the KATRIN experiment [45]: $|\langle m\rangle| < 0.2$ eV (90% C.L.). This corresponds to the following prospective limit on $|\eta_\nu|^2$:

$$|\eta_\nu|^2 \times 10^{10} < 1.6 \times 10^{-3}. \tag{4.5}$$

As the results presented in Section VI indicate, if the limit of 0.2 eV will be reached in the KATRIN experiment, this will lead to severe constraints on some of the solutions for $|\eta_\nu|^2$ obtained in the case of two interfering mechanisms, one of which is the light neutrino exchange.

V. TWO "NONINTERFERING" MECHANISMS

In the case of two active "noninterfering" $(\beta\beta)_{0\nu}$-decay generating mechanisms, which we will assume to be the light LH and heavy RH Majorana neutrino exchanges [27], it is possible to extract the absolute values of the corresponding two LNV fundamental parameters $|\eta_\nu|$ and $|\eta_R|$, using the "data" on the half-lives of two different nuclei undergoing the $(\beta\beta)_{0\nu}$ decay. Indeed, using Eq. (4.1) we can set a system of two linear equations for two unknowns using as input the two half-lives:

$$\begin{aligned}\frac{1}{T_1 G_1} &= |\eta_\nu|^2 |M'^{0\nu}{}_{1,\nu}|^2 + |\eta_R|^2 |M'^{0\nu}{}_{1,N}|^2,\\ \frac{1}{T_2 G_2} &= |\eta_\nu|^2 |M'^{0\nu}{}_{2,\nu}|^2 + |\eta_R|^2 |M'^{0\nu}{}_{2,N}|^2.\end{aligned} \tag{5.1}$$

The solutions read:

$$\begin{aligned}|\eta_\nu|^2 &= \frac{|M'^{0\nu}{}_{2,N}|^2/T_1 G_1 - |M'^{0\nu}{}_{1,N}|^2/T_2 G_2}{|M'^{0\nu}{}_{1,\nu}|^2 |M'^{0\nu}{}_{2,N}|^2 - |M'^{0\nu}{}_{1,N}|^2 |M'^{0\nu}{}_{2,\nu}|^2},\\ |\eta_R|^2 &= \frac{|M'^{0\nu}{}_{1,\nu}|^2/T_2 G_2 - |M'^{0\nu}{}_{2,\nu}|^2/T_1 G_1}{|M'^{0\nu}{}_{1,\nu}|^2 |M'^{0\nu}{}_{2,N}|^2 - |M'^{0\nu}{}_{1,N}|^2 |M'^{0\nu}{}_{2,\nu}|^2}.\end{aligned} \tag{5.2}$$

[3] We remind the reader that for $m_{1,2,3} \gtrsim 0.1$ eV the neutrino mass spectrum is quasidegenerate, $m_1 \cong m_2 \cong m_3 \equiv m$, $m_j^2 \gg \Delta m^2_{21}, |\Delta m^2_{31}|$. In this case we have $m(\bar{\nu}_e) \cong m$ and $|\langle m\rangle| \lesssim m$.

Obviously, solutions giving $|\eta_\nu|^2 < 0$ and/or $|\eta_R|^2 < 0$ are unphysical. Given a pair of nuclei (A_1, Z_1), (A_2, Z_2) of the three ^{76}Ge, ^{100}Mo and ^{130}Te we will be considering, and T_1, and choosing (for convenience) always $A_1 < A_2$, positive solutions for $|\eta_\nu|^2$ and $|\eta_R|^2$ are possible for the following range of values of T_2:

$$\frac{T_1 G_1 |M'^{0\nu}{}_{1,N}|^2}{G_2 |M'^{0\nu}{}_{2,N}|^2} \le T_2 \le \frac{T_1 G_1 |M'^{0\nu}{}_{1,\nu}|^2}{G_2 |M'^{0\nu}{}_{2,\nu}|^2}, \tag{5.3}$$

where we have used the fact that $|M'^{0\nu}{}_{1,\nu}|^2/|M'^{0\nu}{}_{2,\nu}|^2 > |M'^{0\nu}{}_{1,N}|^2/|M'^{0\nu}{}_{2,N}|^2$ (see Table I).[4] Using the values of the phase-space factors and the two relevant NMEs given in Table I in the columns "CD-Bonn, large, $g_A = 1.25$", we get the "positivity" conditions for the ratio of the half-lives of the different pairs of the three nuclei of interest:

$$\begin{aligned}0.15 &\le \frac{T^{0\nu}_{1/2}(^{100}\mathrm{Mo})}{T^{0\nu}_{1/2}(^{76}\mathrm{Ge})} \le 0.18,\\ 0.17 &\le \frac{T^{0\nu}_{1/2}(^{130}\mathrm{Te})}{T^{0\nu}_{1/2}(^{76}\mathrm{Ge})} \le 0.22,\\ 1.14 &\le \frac{T^{0\nu}_{1/2}(^{130}\mathrm{Te})}{T^{0\nu}_{1/2}(^{100}\mathrm{Mo})} \le 1.24.\end{aligned} \tag{5.4}$$

In the case of $g_A = 1.0$ we find:

$$\begin{aligned}0.15 &\le \frac{T^{0\nu}_{1/2}(^{100}\mathrm{Mo})}{T^{0\nu}_{1/2}(^{76}\mathrm{Ge})} \le 0.17,\\ 0.17 &\le \frac{T^{0\nu}_{1/2}(^{130}\mathrm{Te})}{T^{0\nu}_{1/2}(^{76}\mathrm{Ge})} \le 0.23,\\ 1.16 &\le \frac{T^{0\nu}_{1/2}(^{130}\mathrm{Te})}{T^{0\nu}_{1/2}(^{100}\mathrm{Mo})} \le 1.30.\end{aligned} \tag{5.5}$$

It is quite remarkable that the physical solutions are possible only if the ratio of the half-lives of all the pairs of the three isotopes considered take values in very narrow intervals. This result is a consequence of the values of the phase-space factors and of the NME for the two mechanisms considered. In the case of the Argonne potential, large basis and $g_A = 1.25(1.0)$ (see Table I) we get very similar results:

[4] This condition will exhibit a relatively weak dependence on the value of g_A in the cases of mechanisms in which the Gamow-Teller term in the NMEs dominates (as in the gluino exchange dominance and the squark-neutrino exchange mechanisms). Indeed, the factor $(1.25)^4$ (corresponding to $g_A = 1.25$) and included in the definition of the phase-space terms $G_{1,2}$, cancels in the ratio G_1/G_2, and $|M'_{1,\nu(N)}|^2/|M'_{2,\nu(N)}|^2 = |M^{0\nu}{}_{1,\nu(N)}|^2/|M^{0\nu}{}_{2,\nu(N)}|^2$ (see Eq. (2.2)).

$$0.15 \leq \frac{T^{0\nu}_{1/2}(^{100}\mathrm{Mo})}{T^{0\nu}_{1/2}(^{76}\mathrm{Ge})} \leq 0.18,$$
$$0.18 \leq \frac{T^{0\nu}_{1/2}(^{130}\mathrm{Te})}{T^{0\nu}_{1/2}(^{76}\mathrm{Ge})} \leq 0.24(0.25), \quad (5.6)$$
$$1.22 \leq \frac{T^{0\nu}_{1/2}(^{130}\mathrm{Te})}{T^{0\nu}_{1/2}(^{100}\mathrm{Mo})} \leq 1.36(1.42).$$

If it is experimentally established that any of the three ratios of half-lives considered lies outside the interval of physical solutions of $|\eta_\nu|^2$ and $|\eta_R|^2$, obtained taking into account all relevant uncertainties, one would be led to conclude that the $(\beta\beta)_{0\nu}$ decay is not generated by the two mechanisms under discussion. In order to show that the constraints given above are indeed satisfied, the relevant ratios of $(\beta\beta)_{0\nu}$-decay half-lives should be known with a remarkably small uncertainty (not exceeding approximately 5% of the central values of the intervals).

Obviously, given the half-life of one isotope, constraints similar to those described above can be derived on the half-life of any other isotope beyond those considered by us. Similar constraints can be obtained in all cases of two ''noninterfering'' mechanisms generating the $(\beta\beta)_{0\nu}$ decay. The predicted intervals of half-lives of the various isotopes will differ, in general, for the different pairs of ''noninterfering'' mechanisms. However, these differences in the cases of the $(\beta\beta)_{0\nu}$ decay triggered by the exchange of heavy Majorana neutrinos coupled to $(V + A)$ currents and (i) the gluino exchange mechanism, or (ii) the squark-neutrino exchange mechanism, are extremely small. One of the consequences of this feature of the different pairs of ''noninterfering'' mechanisms considered by us is that if it will be possible to rule out one of them as the cause of $(\beta\beta)_{0\nu}$ decay; most likely one will be able to rule out all three of them. The set of constraints under discussion will not be valid, in general, if the $(\beta\beta)_{0\nu}$ decay is triggered by two interfering mechanisms with a non-negligible interference term, or by more than two mechanisms with significant contributions to the $(\beta\beta)_{0\nu}$-decay rates of the different nuclei.

Evidently, if one of the two solutions is zero, for example $|\eta_R|^2 = 0$, then only one of the two $(\beta\beta)_{0\nu}$-decay mechanisms is active. Since for the two mechanisms considered we have $(M'^{0\nu}{}_{1,\nu})^2(M'^{0\nu}{}_{2,N})^2 - (M'^{0\nu}{}_{1,N})^2 \times (M'^{0\nu}{}_{2,\nu})^2 \neq 0$, the condition that $|\eta_R|^2 = 0$ reads:

$$|M'^{0\nu}{}_{1,\nu}|^2 T_1 G_1 = |M'^{0\nu}{}_{2,\nu}|^2 T_2 G_2, \quad |\eta_R|^2 = 0. \quad (5.7)$$

The condition that $|\eta_\nu|^2 = 0$ has a similar form:

$$|M'^{0\nu}{}_{1,N}|^2 T_1 G_1 = |M'^{0\nu}{}_{2,N}|^2 T_2 G_2, \quad |\eta_\nu|^2 = 0. \quad (5.8)$$

If only the light neutrino exchange mechanism is present and the NMEs are correctly calculated, the $(\beta\beta)_{0\nu}$-decay effective Majorana mass (and $|\eta_\nu|^2$) extracted from all three (or any number of) $(\beta\beta)_{0\nu}$-decay isotopes must be the same (see, e.g., [46,47]). Similarly, if the heavy RH Majorana neutrino exchange gives the dominant contribution, the extracted value $|\eta_R|^2$ must be the same for all three (or more) $(\beta\beta)_{0\nu}$-decay nuclei.

We analyze next the possible solutions for different combinations of the half-lives of the following isotopes: ^{76}Ge, ^{100}Mo and ^{130}Te. Assuming the half-lives of two isotopes to be known and using the physical solutions for $|\eta_\nu|^2$ and $|\eta_R|^2$ obtained using these half-lives, one can obtain a prediction for the half-life of the third isotope. The predicted half-life should satisfy the existing lower limits on it. In the calculations the results of which are reported here, we fixed the half-life of one of the two isotopes and assumed the second half-life lies in an interval compatible with the existing constraints. We used the value of $T^{0\nu}_{1/2}(^{76}\mathrm{Ge})$ and values of $T^{0\nu}_{1/2}(^{100}\mathrm{Mo})$ and $T^{0\nu}_{1/2}(^{130}\mathrm{Te})$ from the intervals given in (4.3). The system of two equations is solved and the values of $|\eta_\nu|^2 > 0$ and $|\eta_R|^2 > 0$ thus obtained were used to obtain predictions for the half-life of the third isotope. The results for NMEs corresponding to the case ''CD-Bonn, large, $g_A = 1.25$'' (see Table I) are given in Table II. We note that the experimental lower bounds quoted in Eq. (4.3) have to be taken into account since they can further constrain the range of allowed values of $|\eta_\nu|^2$ and $|\eta_R|^2$. Indeed, an inspection of the values in Table II shows that not all the ranges predicted for the third half-life using the solutions obtained for $|\eta_R|^2$ and $|\eta_\nu|^2$ are compatible with the lower bounds on the half-lives of the considered nuclear isotopes, given in (4.3). In this case, some or all ''solution'' values of $|\eta_R|^2$ and/or $|\eta_\nu|^2$ are ruled out. In Table II these cases are marked by a star.

The results reported in Table II are stable with respect to variations of the NMEs. If we use the NMEs corresponding to the case ''CD-Bonn, large, $g_A = 1.0$'' (see Table I), the limits of the intervals quoted in Table II change by $\pm 5\%$. If instead we use the NMEs corresponding to the Argonne potential, large basis and $g_A = 1.25$ ($g_A = 1.0$), the indicated limits change by $\pm 10\%$ ($\pm$ 14%).

These results and considerations are illustrated in Figs. 3–7. The horizontal dashed line in these figures corresponds to the prospective limit planned to be obtained in the upcoming KATRIN experiment [45]. In Fig. 3 we show the solutions for $|\eta_R|^2$ and/or $|\eta_\nu|^2$ (conveniently rescaled), obtained for two values of $T^{0\nu}_{1/2}(^{76}\mathrm{Ge}) = 2.23 \times 10^{25}$ y and 10^{26} y, assuming $T^{0\nu}_{1/2}(^{100}\mathrm{Mo})$ has a value in a certain interval. In the case of $T^{0\nu}_{1/2}(^{76}\mathrm{Ge}) = 2.23 \times 10^{25}$ and $T^{0\nu}_{1/2}(^{76}\mathrm{Ge}) = 10^{26}$ y, the derived physical values of $|\eta_R|^2$ and $|\eta_\nu|^2$ lead to predictions for $T^{0\nu}_{1/2}(^{100}\mathrm{Te})$ which are compatible with the existing lower limit (Fig. 3, left and right panel). We get similar results using as input in the system of two equations for $|\eta_R|^2$ and $|\eta_\nu|^2$ the half-lives of different pairs of isotopes, and the lower limit of the half-life

TABLE II. The predictions for the half-life of a third nucleus (A_3, Z_3), using as input in the system of equations for $|\eta_\nu|^2$ and $|\eta_R|^2$, Eq. (5.1), the half-lives of two other nuclei (A_1, Z_1) and (A_2, Z_2). The three nuclei used are ^{76}Ge, ^{100}Mo and ^{130}Te. The results shown are obtained for a fixed value of the half-life of (A_1, Z_1) and assuming the half-life of (A_2, Z_2) to lie in a certain specific interval. The physical solutions for $|\eta_\nu|^2$ and $|\eta_R|^2$ are then used to derive predictions for the half-life of the third nucleus (A_3, Z_3). The latter are compared with the lower limits given in Eq. (4.3). The results quoted are obtained for NMEs given in the columns "CD-Bonn, large, $g_A = 1.25$" in Table I. One star beside the isotope pair whose half-lives are used as input for the system of equations (5.1), indicates predicted ranges of half-lives of the nucleus (A_3, Z_3) that are not compatible with the lower bounds given in (4.3).

Pair	$T^{0\nu}_{1/2}(A_1, Z_1)$ [yr]	$T^{0\nu}_{1/2}[A_2, Z_2]$ [yr]	Prediction on $[A_3, Z_3]$ [yr]
^{76}Ge − ^{100}Mo	$T(\mathrm{Ge}) = 2.23 \times 10^{25}$	$3.23 \times 10^{24} \leq T(\mathrm{Mo}) \leq 3.97 \times 10^{24}$	$3.68 \times 10^{24} \leq T(\mathrm{Te}) \leq 4.93 \times 10^{24}$
^{76}Ge − ^{130}Te	$T(\mathrm{Ge}) = 2.23 \times 10^{25}$	$3.68 \times 10^{24} \leq T(\mathrm{Te}) \leq 4.93 \times 10^{24}$	$3.23 \times 10^{24} \leq T(\mathrm{Mo}) \leq 3.97 \times 10^{24}$
^{76}Ge − ^{100}Mo	$T(\mathrm{Ge}) = 10^{26}$	$1.45 \times 10^{25} \leq T(\mathrm{Mo}) \leq 1.78 \times 10^{25}$	$1.65 \times 10^{25} \leq T(\mathrm{Te}) \leq 2.21 \times 10^{25}$
^{76}Ge − ^{130}Te	$T(\mathrm{Ge}) = 10^{26}$	$1.65 \times 10^{25} \leq T(\mathrm{Te}) \leq 2.21 \times 10^{25}$	$1.45 \times 10^{25} \leq T(\mathrm{Mo}) \leq 1.78 \times 10^{25}$
^{100}Mo − ^{130}Te ⋆	$T(\mathrm{Mo}) = 5.8 \times 10^{23}$	$6.61 \times 10^{23} \leq T(\mathrm{Te}) \leq 7.20 \times 10^{23}$	$3.26 \times 10^{24} \leq T(\mathrm{Ge}) \leq 4.00 \times 10^{24}$
^{100}Mo − ^{130}Te	$T(\mathrm{Mo}) = 4 \times 10^{24}$	$4.56 \times 10^{24} \leq T(\mathrm{Te}) \leq 4.97 \times 10^{24}$	$2.25 \times 10^{25} \leq T(\mathrm{Ge}) \leq 2.76 \times 10^{25}$
^{100}Mo − ^{130}Te	$T(\mathrm{Mo}) = 5.8 \times 10^{24}$	$6.61 \times 10^{24} \leq T(\mathrm{Te}) \leq 7.20 \times 10^{24}$	$3.26 \times 10^{25} \leq T(\mathrm{Ge}) \leq 4.00 \times 10^{25}$
^{100}Mo − ^{130}Te ⋆	$T(\mathrm{Te}) = 3 \times 10^{24}$	$2.42 \times 10^{24} \leq T(\mathrm{Mo}) \leq 2.63 \times 10^{24}$	$1.36 \times 10^{25} \leq T(\mathrm{Ge}) \leq 1.82 \times 10^{25}$
^{100}Mo − ^{130}Te	$T(\mathrm{Te}) = 1.65 \times 10^{25}$	$1.33 \times 10^{25} \leq T(\mathrm{Mo}) \leq 1.45 \times 10^{25}$	$7.47 \times 10^{25} \leq T(\mathrm{Ge}) \leq 1.00 \times 10^{26}$
^{100}Mo − ^{130}Te	$T(\mathrm{Te}) = 3 \times 10^{25}$	$2.42 \times 10^{25} \leq T(\mathrm{Mo}) \leq 2.63 \times 10^{25}$	$1.36 \times 10^{26} \leq T(\mathrm{Ge}) \leq 1.82 \times 10^{26}$

of the third as an additional constraint. They are presented in Figs. 4–6. In Fig. 7 we show the solutions for $|\eta_\nu|^2$ and $|\eta_R|^2$ for $T^{0\nu}_{1/2}(^{130}\mathrm{Te}) = 3 \times 10^{24}$ y and $T^{0\nu}_{1/2}(^{100}\mathrm{Mo}) = (2.42\text{–}2.63) \times 10^{24}$ y. In contrast to the cases illustrated in Figs. 3–6, most of the solution values of $|\eta_\nu|^2$ and $|\eta_R|^2$ are excluded by taking into account the lower bound on $T^{0\nu}_{1/2}(^{76}\mathrm{Ge})$ given in Eq. (4.3).

We have also studied the dependence of the results discussed above on the value of g_A and the NMEs used. This was done using the large basis NMEs, obtained with the CD-Bonn and Argonne potentials for the two values of $g_A = 1.25$, 1.0. Some of the results of this study are presented graphically in Figs. 8 and 9. The horizontal dashed line in these two figures corresponds again to the prospective limit from the upcoming KATRIN experiment [45]. We note that in the cases studied by us, changing the value of g_A from 1.25 to 1.0 for a given potential (CD-Bonn or Argonne) does not lead to a significant change of the solutions for $|\eta_\nu|^2$ and $|\eta_R|^2$: the change is smaller than approximately 10%. The solutions exhibit a larger variation when for a given g_A and basis, the NMEs calculated with the CD-Bonn potential are replaced by the NME's obtained with the Argonne potential (Fig. 9, upper right and lower left panels). In this case, as we have mentioned earlier, given T_1, the interval of allowed values of the half-life of the second nucleus T_2 changes somewhat. In

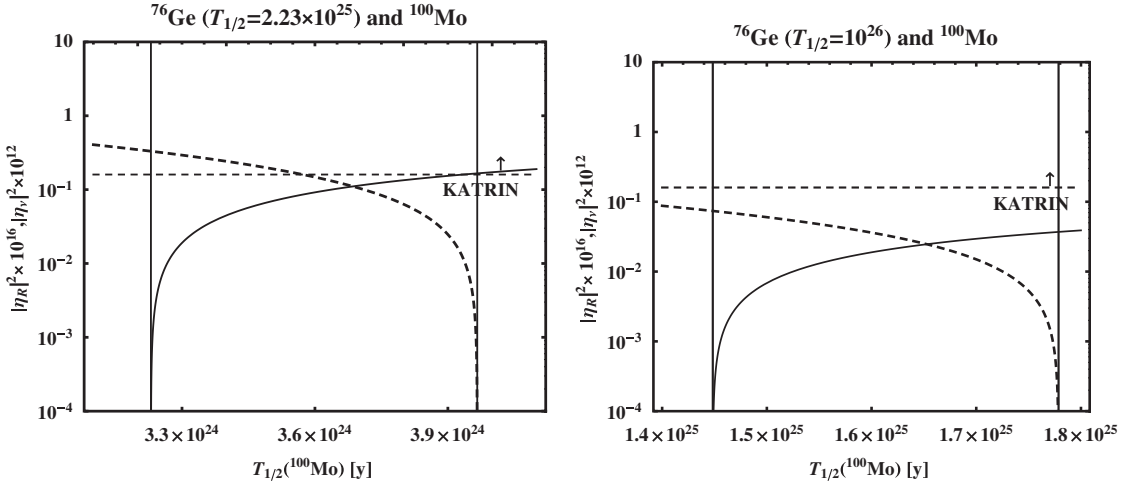

FIG. 3. The values of the rescaled parameters $|\eta_\nu|^2$ (solid line) and $|\eta_R|^2$ (dashed lined), obtained as solutions of Eq. (5.1) for two values of $T^{0\nu}_{1/2}(^{76}\mathrm{Ge})$ and values of $T^{0\nu}_{1/2}(^{100}\mathrm{Mo})$ lying in a specific interval. The physical (positive) solutions are delimited by the two vertical lines. The lower bound on $T^{0\nu}_{1/2}(^{130}\mathrm{Te})$ given in (4.3) does not lead to further constraints on $|\eta_\nu|^2$ and $|\eta_R|^2$. The horizontal dashed line corresponds to the prospective upper limit from the upcoming ^3H β-decay experiment KATRIN [45]. See text for further details.

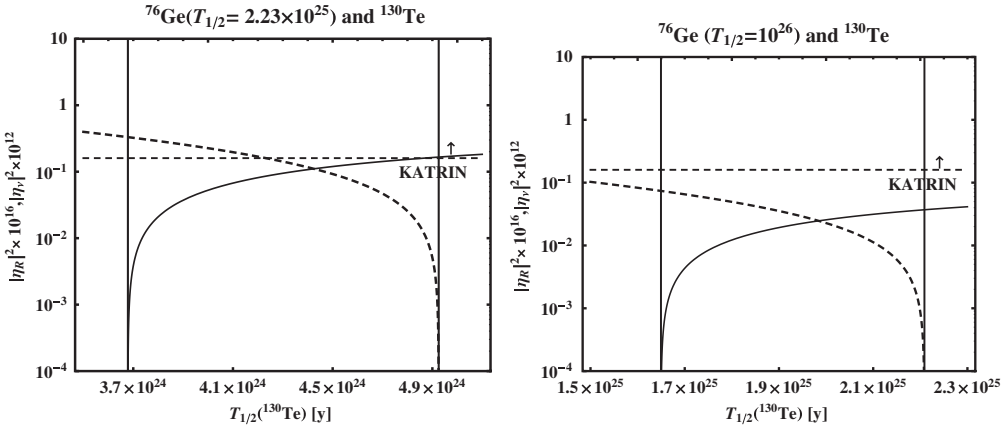

FIG. 4. The same as in Fig. 3, but using as input hypothetical values of the half-lives of ^{76}Ge and ^{130}Te, $T^{0\nu}_{1/2}(^{76}\text{Ge})$ and $T^{0\nu}_{1/2}(^{130}\text{Te})$. The physical (positive) solutions are delimited by the two vertical lines. The lower bound on $T^{0\nu}_{1/2}(^{100}\text{Mo})$ given in (4.3) does not lead to further constraints on $|\eta_{\nu,R}|^2$.

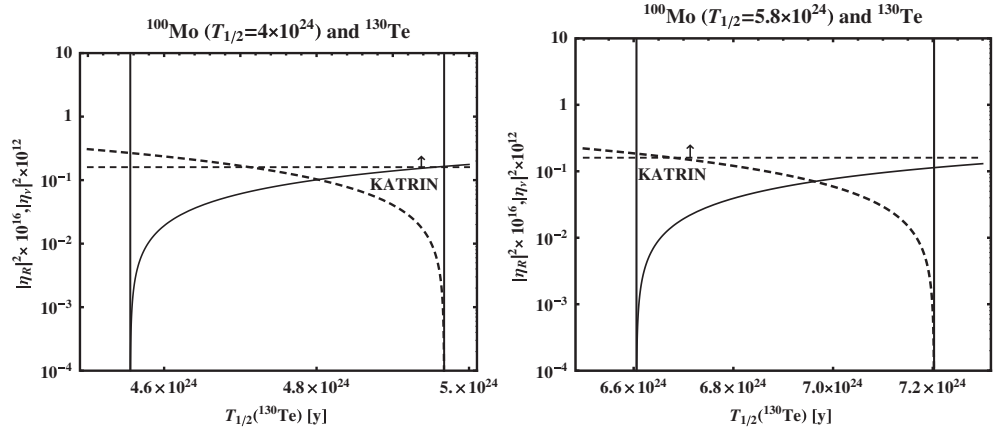

FIG. 5. The same as in Fig. 3, but using as input two values of the half-life of ^{100}Mo and values of the half-life of ^{130}Te lying in a specific interval. The physical (positive) solutions are delimited by the two vertical lines. The lower bound on $T^{0\nu}_{1/2}(^{76}\text{Ge})$ given in (4.3) does not lead to further constraints on $|\eta_\nu|^2$ and $|\eta_R|^2$.

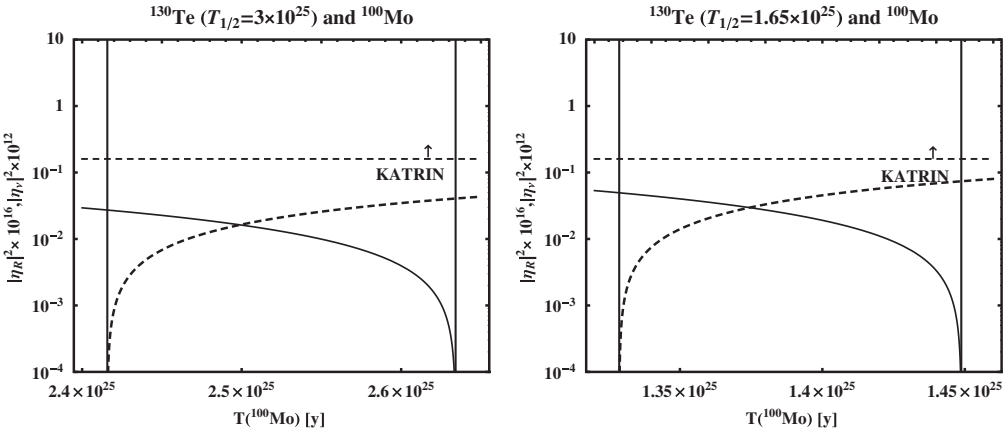

FIG. 6. The same as in Fig. 5, but using as input two values of the half-life of ^{130}Te and values of the half-life of ^{100}Mo lying in a specific interval. The physical (positive) solutions are delimited by the two thick vertical lines. The lower bound on $T^{0\nu}_{1/2}(^{76}\text{Ge})$ does not lead to further constraints on $|\eta_\nu|^2$ and $|\eta_R|^2$.

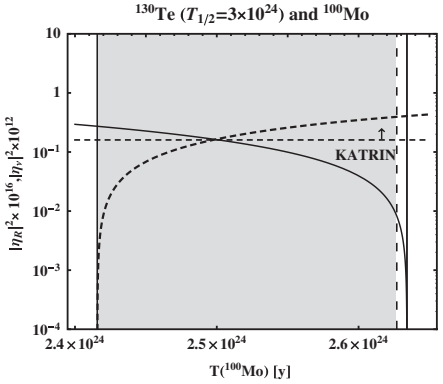

FIG. 7. The values of the rescaled parameters $|\eta_\nu|^2$ (solid line) and $|\eta_R|^2$ (dashed lined), obtained as solutions of Eq. (5.1) for the minimum value of $T^{0\nu}_{1/2}(^{130}\mathrm{Te})$ specified in Eq. (4.3). The physical (positive) solutions are delimited by the two vertical lines. The gray region is an excluded due to the lower bound on $T^{0\nu}_{1/2}(^{76}\mathrm{Ge})$ quoted in (4.3).

the specific cases shown, e.g., in Fig. 9 (upper right and lower left panels), $T_1 \equiv T^{0\nu}_{1/2}(^{76}\mathrm{Ge}) = 2.23 \times 10^{25}$ y and the interval of interest of values of $T_2 \equiv T^{0\nu}_{1/2}(^{100}\mathrm{Mo})$ shifts to larger values. Obviously, the solution values of the parameters $|\eta_\nu|^2$ and $|\eta_R|^2$, obtained with the two different sets of the NMEs, can differ drastically in the vicinity of the maximum and minimum values of T_2, as is also seen in Figs. 8 and 9. If a given extreme value of T_2, say $\max(T_2)$, obtained with one set of NMEs, belongs to the interval of allowed values of T_2, found with a second set of NMEs, one of the fundamental parameters, calculated at $\max(T_2)$ with the first set of NMEs can be zero, and can have a relatively large nonzero value when calculated with the second set of NMEs. Moreover, there are narrow intervals of values of T_2 for which there exist physical solutions for $|\eta_\nu|^2$ and $|\eta_R|^2$ if one uses the NMEs obtained with the CD-Bonn potential and there are no physical solutions for the NMEs derived with the Argonne potential. If the

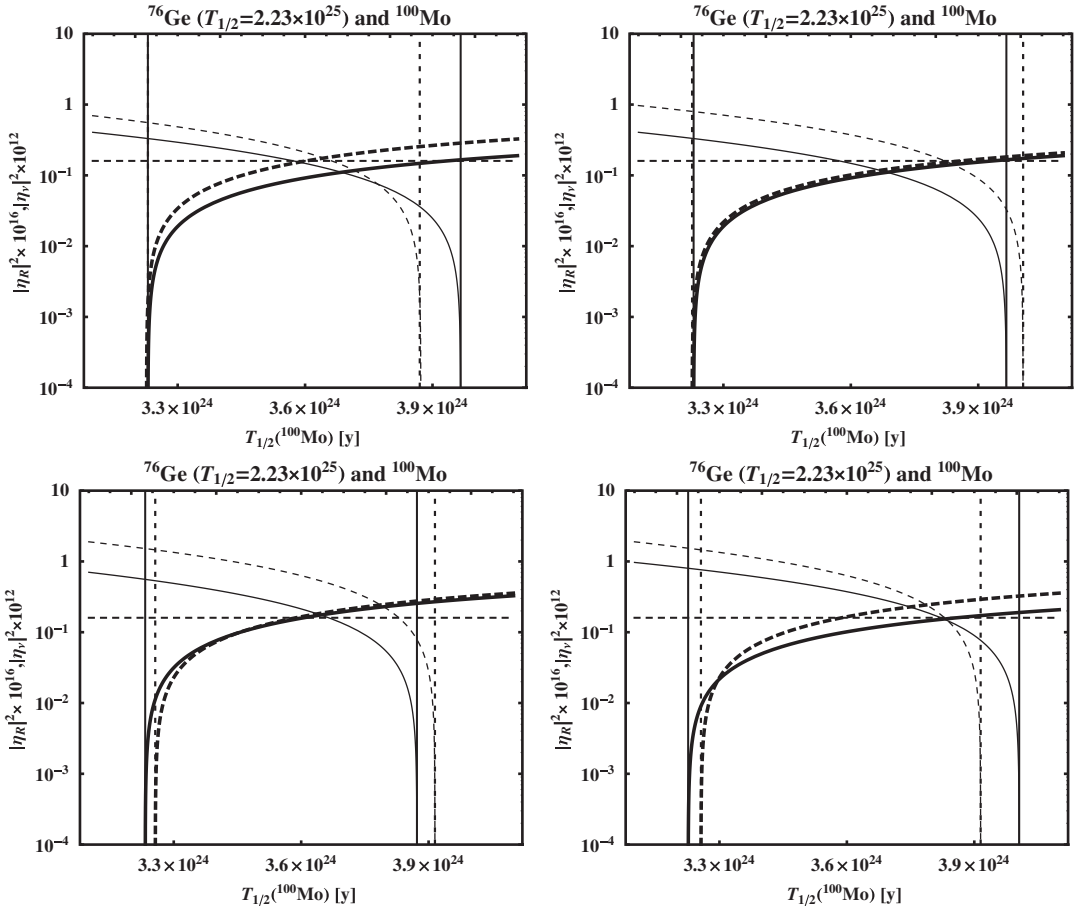

FIG. 8. Solutions for $|\eta_\nu|^2$ (thick lines) and $|\eta_R|^2$ (thin lines), obtained by fixing $T_1 = T^{0\nu}_{1/2}(^{76}\mathrm{Ge}) = 2.23 \times 10^{25}$ yr and $T_2 = T^{0\nu}_{1/2}(^{100}\mathrm{Mo})$ and using the sets of NMEs calculated using the large basis and (i) CD-Bonn potential, $g_A = 1.25$ (solid lines) and $g_A = 1$ (dashed lines) (upper left panel); (ii) CD-Bonn (solid lines) and Argonne (dashed lines) potentials with $g_A = 1.25$ (upper right panel); (iii) CD-Bonn (solid lines) and Argonne (dashed lines) potentials with $g_A = 1.0$ (lower left panel); (iv) Argonne potential with $g_A = 1.25$ (solid lines) and $g_A = 1$ (dashed lines) (lower right panel). The physical (positive) solutions for $|\eta_\nu|^2$ and $|\eta_R|^2$ shown with solid (dashed) lines are delimited by two vertical solid (dashed) lines. The horizontal dashed line corresponds to the prospective upper limit [45] $|\langle m\rangle| < 0.2$ eV.

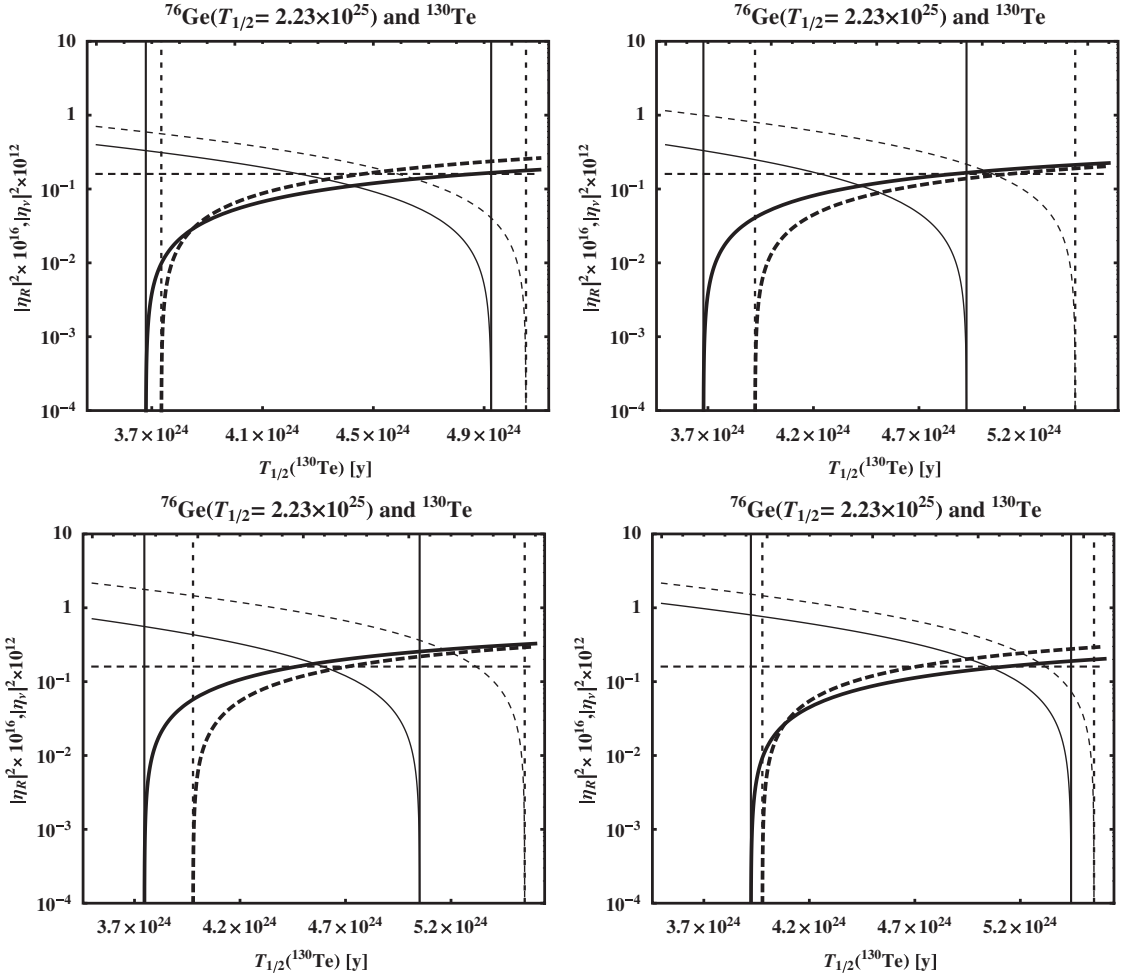

FIG. 9. The same as in Fig. 8, but for $T_1 = T^{0\nu}_{1/2}(^{76}\text{Ge}) = 2.23 \times 10^{25}$ yr and $T_2 = T^{0\nu}_{1/2}(^{130}\text{Te})$.

measured value of T_2 falls in such an interval, this can imply that either the two mechanisms considered are not at work in $(\beta\beta)_{0\nu}$ decay, or one of the two sets of NMEs does not describe correctly the nuclear transitions. As Figs. 8 and 9 indicate, the data from the KATRIN experiment can help limit further the solutions for $|\eta_\nu|^2$, obtained with NMEs calculated with the CD-Bonn potential and $g_A = 1.0$ or with the Argonne potential.

Let us note finally that Figs. 8 and 9 were obtained using hypothetical half-lives of ^{76}Ge and ^{100}Mo. We get similar results if we use as input hypothetical half-lives of a different pair of nuclei, ^{76}Ge and ^{130}Te, ^{130}Te and ^{100}Mo, etc.

VI. TWO INTERFERING MECHANISMS

Neutrinoless double beta decay can be triggered by two competitive mechanisms whose interference contribution to the $(\beta\beta)_{0\nu}$-decay rates is non-negligible. In this Section we analyze the case of light Majorana neutrino exchange and gluino exchange. From Eq. (4.2) it is possible to extract

TABLE III. Ranges of half-lives of T_3 in the case of two interfering mechanisms: the light Majorana neutrino exchange and gluino exchange dominance.

$T^{0\nu}_{1/2}$ [y] (fixed)	$T^{0\nu}_{1/2}$ [y](fixed)	Allowed
$T(\text{Ge}) = 2.23 \times 10^{25}$	$T(\text{Mo}) = 5.8 \times 10^{24}$	$5.99 \times 10^{24} \leq T(\text{Te}) \leq 7.35 \times 10^{24}$
$T(\text{Ge}) = 2.23 \times 10^{25}$	$T(\text{Te}) = 3 \times 10^{24}$	$2.46 \times 10^{24} \leq T(\text{Mo}) \leq 2.82 \times 10^{24}$
$T(\text{Ge}) = 10^{26}$	$T(\text{Mo}) = 5.8 \times 10^{24}$	$6.30 \times 10^{24} \leq T(\text{Te}) \leq 6.94 \times 10^{24}$
$T(\text{Ge}) = 10^{26}$	$T(\text{Te}) = 3 \times 10^{24}$	$2.55 \times 10^{24} \leq T(\text{Mo}) \leq 2.72 \times 10^{24}$
$T(\text{Ge}) = 2.23 \times 10^{25}$	$T(\text{Te}) = 3 \times 10^{25}$	$2.14 \times 10^{25} \leq T(\text{Mo}) \leq 3.31 \times 10^{25}$
$T(\text{Ge}) = 10^{26}$	$T(\text{Te}) = 3 \times 10^{25}$	$2.38 \times 10^{25} \leq T(\text{Mo}) \leq 2.92 \times 10^{25}$

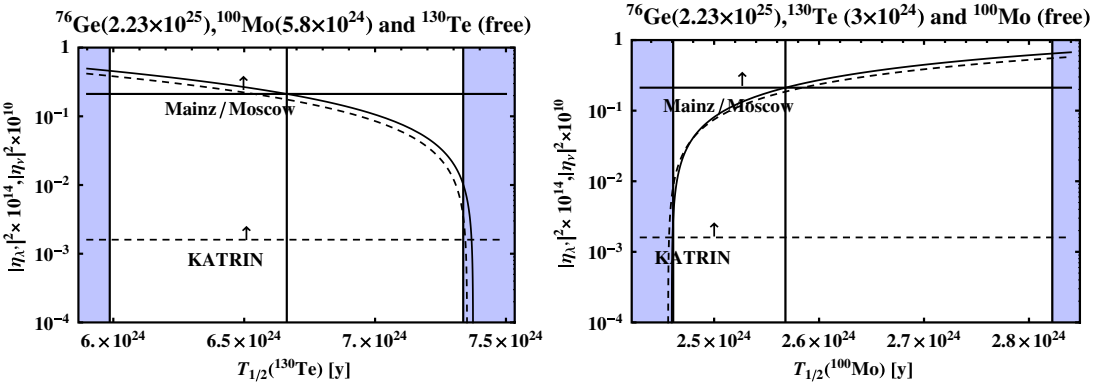

FIG. 10 (color online). The values of the rescaled parameters $|\eta_\nu|^2$ (thick line) and $|\eta_{\lambda'}|^2$ (dashed lined), obtained as solutions of the system of equations (4.2) for fixed values of $T^{0\nu}_{1/2}(^{76}\text{Ge})$ and $T^{0\nu}_{1/2}(^{100}\text{Mo})$ and values of $T^{0\nu}_{1/2}(^{130}\text{Te})$ lying in a specific interval. The physical allowed regions correspond to the areas shown in white, while the areas shown in gray are excluded. The horizontal solid (dashed) line corresponds to the upper limit [44,45] $|\langle m\rangle| < 2.3$ eV (prospective upper limit [45] $|\langle m\rangle| < 0.2$ eV). See text for details.

the values of $|\eta_\nu|^2$, $|\eta_{\lambda'}|^2$ and $\cos\alpha$ setting up a system of three equations with these three unknowns using as input the data on the half-lives of three different nuclei. The solutions are given by:

$$|\eta_\nu|^2 = \frac{D_1}{D}, \qquad |\eta_{\lambda'}|^2 = \frac{D_2}{D}, \qquad z \equiv 2\cos\alpha|\eta_\nu||\eta_{\lambda'}| = \frac{D_3}{D}, \tag{6.1}$$

where D, D_1, D_2 and D_3 are the following determinants

$$D = \begin{vmatrix} (M^{0\nu}_{1,\nu})^2 & (M^{0\nu}_{1,\lambda'})^2 & M^{0\nu}_{1,\lambda'}M^{0\nu}_{1,\nu} \\ (M^{0\nu}_{2,\nu})^2 & (M^{0\nu}_{2,\lambda'})^2 & M^{0\nu}_{2,\lambda'}M^{0\nu}_{2,\nu} \\ (M^{0\nu}_{3,\nu})^2 & (M^{0\nu}_{3,\lambda'})^2 & M^{0\nu}_{3,\lambda'}M^{0\nu}_{3,\nu} \end{vmatrix},$$

$$D_1 = \begin{vmatrix} 1/T_1G_1 & (M^{0\nu}_{1,\lambda'})^2 & M^{0\nu}_{1,\lambda'}M^{0\nu}_{1,\nu} \\ 1/T_2G_2 & (M^{0\nu}_{2,\lambda'})^2 & M^{0\nu}_{2,\lambda'}M^{0\nu}_{2,\nu} \\ 1/T_3G_3 & (M^{0\nu}_{3,\lambda'})^2 & M^{0\nu}_{3,\lambda'}M^{0\nu}_{3,\nu} \end{vmatrix}, \tag{6.2}$$

$$D_2 = \begin{vmatrix} (M^{0\nu}_{1,\nu})^2 & 1/T_1G_1 & M^{0\nu}_{1,\lambda'}M^{0\nu}_{1,\nu} \\ (M^{0\nu}_{2,\nu})^2 & 1/T_2G_2 & M^{0\nu}_{2,\lambda'}M^{0\nu}_{2,\nu} \\ (M^{0\nu}_{3,\nu})^2 & 1/T_3G_3 & M^{0\nu}_{3,\lambda'}M^{0\nu}_{3,\nu} \end{vmatrix},$$

$$D_3 = \begin{vmatrix} (M^{0\nu}_{1,\nu})^2 & (M^{0\nu}_{1,\lambda'})^2 & 1/T_1G_1 \\ (M^{0\nu}_{2,\nu})^2 & (M^{0\nu}_{2,\lambda'})^2 & 1/T_2G_2 \\ (M^{0\nu}_{3,\nu})^2 & (M^{0\nu}_{3,\lambda'})^2 & 1/T_3G_3 \end{vmatrix}. \tag{6.3}$$

We must require that $|\eta_\nu|^2$ and $|\eta_{\lambda'}|^2$ be non-negative and that the factor $2\cos\alpha|\eta_\nu||\eta_{\lambda'}|$ in the interference term satisfies:

$$-2|\eta_\nu||\eta_{\lambda'}| \le 2\cos\alpha|\eta_\nu||\eta_{\lambda'}| \le 2|\eta_\nu||\eta_{\lambda'}|. \tag{6.4}$$

If we fix (i.e., have data on) the half-lives of two of the nuclei and combine these with the condition in Eq. (6.4), we can obtain the interval of values of the half-life of the third nucleus, which is compatible with the data on the half-lives of the two other nuclei and the mechanisms considered. The minimal (maximal) value of this interval of half-lives of the third nucleus is obtained for $\cos\alpha = +1$ ($\cos\alpha = -1$). Examples of the intervals of half-life values of the third nucleus obtained using the half-life values of the other two nuclei [5] for the $(\beta\beta)_{0\nu}$-decay mechanisms discussed are listed in Table III. The results reported in Table III are obtained with NMEs corresponding to the CD-Bonn potential, the large basis and $g_A = 1.25$.

We show in a few illustrative figures (Figs. 10–13) the results of the determination of $|\eta_\nu|^2$, $|\eta_{\lambda'}|^2$ and $\cos\alpha$ using different values of half-lives of the three nuclei ^{76}Ge, ^{100}Mo and ^{130}Te from the intervals given in Eq. (4.3). The lower bounds of the half-lives quoted in Eq. (4.3) are taken into account. In these figures the physical allowed regions correspond to the areas shown in white, while the areas shown in gray are excluded. The allowed interval of values of the half-life of the 3rd nucleus, corresponding to the white areas, are listed in the 3rd column of Table III. The results presented in Figs. 10–13 are derived using the NMEs, calculated with the CD-Bonn potential, the large basis and $g_A = 1.25$.

It is interesting to note that for the two fixed half-life values used to obtain Figs. 10–12, the interference between the contributions of the two mechanisms considered is destructive: one finds using these values that for most of the physical (positive) solutions for $|\eta_\nu|^2$ and $|\eta_{\lambda'}|^2$, $\cos\alpha$ is negative. Moreover, the rescaled parameters

[5]Technically this is done in the following way. Fixing the half-lives of two isotopes, T_1 and T_2, and varying the half-life of the third isotope T_3 in a certain interval, we obtained $|\eta_\nu|^2$, $|\eta_{\lambda'}|^2$ and $z = 2\cos\alpha|\eta_\nu||\eta_{\lambda'}|$ as a function of T_3. Requiring that $|\eta_\nu|^2 > 0$, $|\eta_{\lambda'}|^2 > 0$ and that $-2\eta_\nu||\eta_{\lambda'}| \le z \le 2\eta_\nu||\eta_{\lambda'}|$ determines the interval of physically allowed values of T_3 (given T_1, T_2 and the mechanisms of $(\beta\beta)_{0\nu}$ decay considered). This interval of physically allowed values of T_3 is shown in Table III.

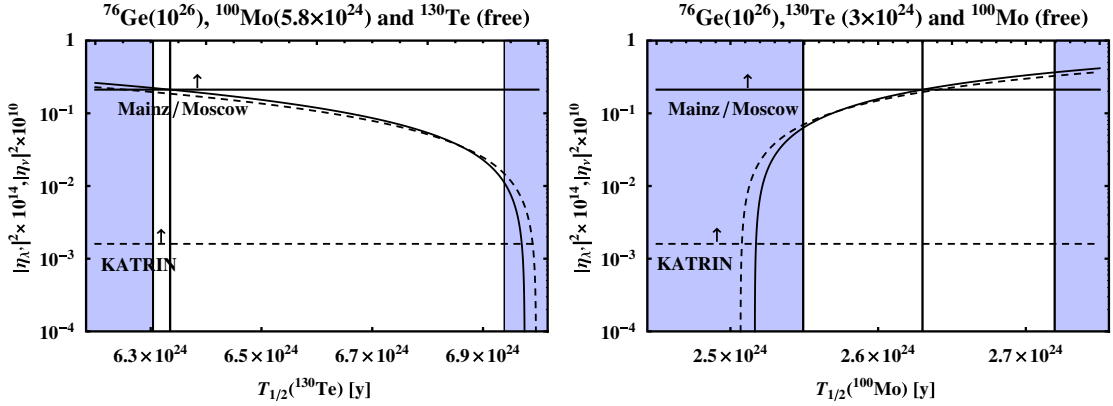

FIG. 11 (color online). The same as in Fig. 10 for a different set of values of the three half-lives used as input in the analysis.

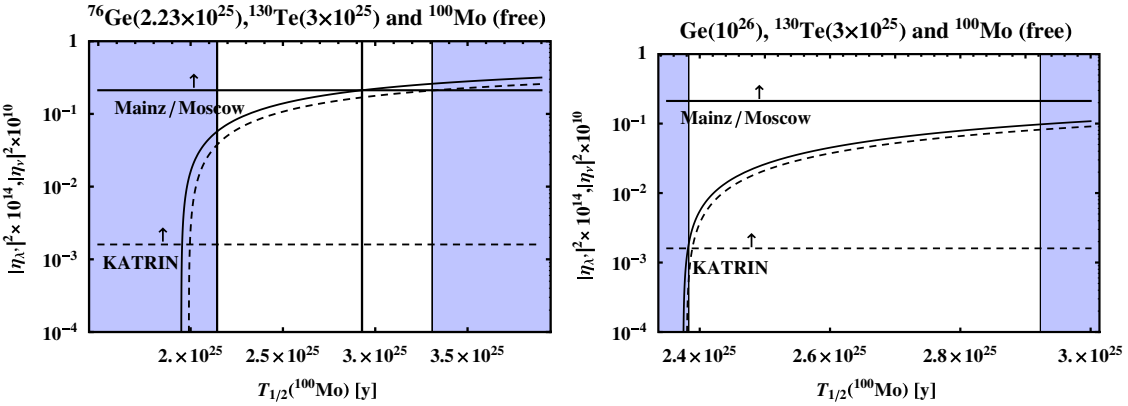

FIG. 12 (color online). The same as in Figs. 10 and 11 for a different set of values of the three half-lives used as input in the analysis.

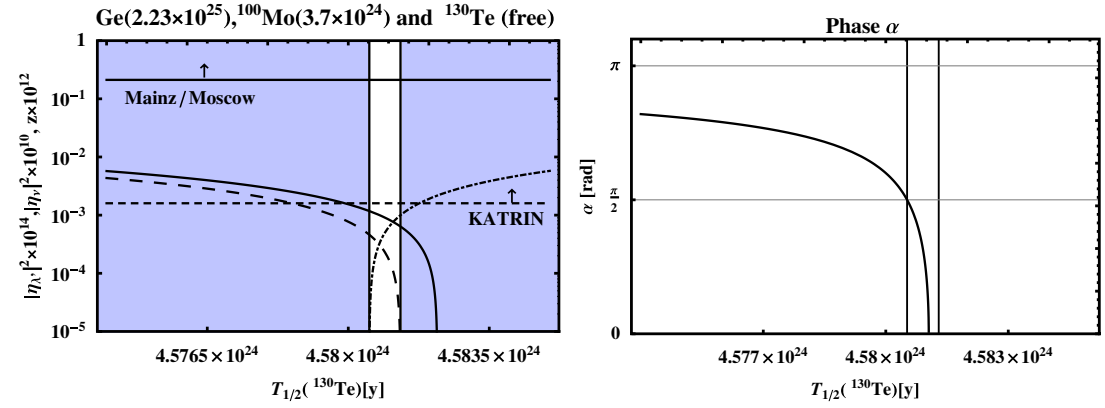

FIG. 13 (color online). Left Panel: the values of $|\eta_\nu|^2 \times 10^{10}$ (thick line), $|\eta_{\lambda'}|^2 \times 10^{14}$ (dashed line) and $z = 2\cos\alpha|\eta_\nu||\eta_{\lambda'}| \times 10^{12}$ (dot-dashed line) corresponding to the half-lives of ^{76}Ge, ^{100}Mo and ^{130}Te indicated on the figure. The interval of values of $T^{0\nu}_{1/2}(^{130}\text{Te})$ between the two vertical lines corresponds to physical (positive) solutions for $|\eta_\nu|^2$ and $|\eta_{\lambda'}|^2$ as well as to a positive z (i.e., to a constructive interference between the contributions due to the two mechanisms). The horizontal solid (dashed) line corresponds to the upper limit [44,45] $|\langle m\rangle| < 2.3$ eV (prospective upper limit [45] $|\langle m\rangle| < 0.2$ eV). See text for details. Right Panel: the phase α.

$|\eta_\nu|^2 \times 10^{10}$ and $|\eta_{\lambda'}|^2 \times 10^{14}$ in most of the solution regions have very close values. This is due to the fact that for most of the physically allowed values of $|\eta_\nu|^2$ and $|\eta_{\lambda'}|^2$, each of the two terms including $|\eta_\nu|^2$ or $|\eta_{\lambda'}|^2$ as a factor in the right hand side of Eq. (4.2) is much larger than the free term in the left hand side of Eq. (4.2). As a consequence, in order to explain the data (i.e., the chosen values of the half-lives of the three isotopes) there should be a strong mutual compensation between the contributions due to the two mechanisms. This is possible only if $|\eta_\nu|^2 (M^{0\nu}_{i,\nu})^2$ and $|\eta_{\lambda'}|^2 (M^{0\nu}_{i,\lambda'})^2$ have close values and $\cos\alpha \cong -1$.

In the case of destructive interference between the two contributions, $|\langle m \rangle|$ can have values which exceed the limit on the absolute scale of neutrino masses set by the ^3H β-decay experiments [44,45], Eq. (4.4). This limit is indicated as a horizontal solid line in Figs. 10–12. It leads to further constraints on the physical solution for $|\eta_\nu|^2$, and thus for $|\eta_{\lambda'}|^2$.

As we have already indicated, a more stringent limit on the absolute neutrino mass scale and therefore on $|\langle m \rangle|$ is planned to be obtained in the KATRIN experiment [45]: it is given in Eq. (4.5). The KATRIN prospective upper bound is shown as a horizontal dashed line in Figs. 10–12. As the results presented in Figs. 10–12 indicate, if the limit of 0.2 eV will be reached in the KATRIN experiment, it will lead to severe constraints on the solutions for $|\eta_\nu|^2$ obtained in the cases we have considered, strongly disfavoring (if not ruling out) essentially all of them.

In Fig. 13 we illustrate the possibility of constructive interference between the light neutrino and the gluino exchange contributions. The solutions shown in Fig. 13 are not constrained by the limits obtained in the ^3H β-decay experiments [44,45]; they also satisfy the prospective upper limit from the KATRIN experiment.

It is not difficult to derive from Eqs. (6.1), (6.2), and (6.3) the general conditions under which $|\eta_\nu|^2$ and $|\eta_{\lambda'}|^2$ are positive and the interference between the light neutrino and gluino exchange contributions is constructive (destructive), i.e., $\cos\alpha$ (or z) is positive (negative). We will illustrate them later using again the NMEs calculated with the CD-Bonn potential, the large basis and $g_A = 1.25$.

Consider first the conditions for constructive interference. We will introduce a somewhat simplified notation in this part of the article: T_i, G_i, M_i and Λ_i for $i = 1, 2, 3$ will denote, respectively, the half-life, phase-space factor, light neutrino and dominant gluino exchange NMEs for ^{76}Ge ($i = 1$), ^{100}Mo ($i = 2$) and ^{130}Te ($i = 3$). The first thing to notice is that it follows from Table I that the ratios of NMEs M_i/Λ_i satisfy the inequalities:

$$\frac{M_1}{\Lambda_1} > \frac{M_2}{\Lambda_2} > \frac{M_3}{\Lambda_3}. \tag{6.5}$$

This implies that the determinant D, defined in Eq. (6.2), is negative:

$$D = \Lambda_1^2 \Lambda_2^2 \Lambda_3^2 \left(\frac{M_2}{\Lambda_2} - \frac{M_1}{\Lambda_1}\right)\left(\frac{M_3}{\Lambda_3} - \frac{M_1}{\Lambda_1}\right)\left(\frac{M_3}{\Lambda_3} - \frac{M_2}{\Lambda_2}\right). \tag{6.6}$$

Consequently, in order to have $|\eta_\nu|^2 >$, $|\eta_{\lambda'}|^2 > 0$ and constructive interference between the two contributions, i.e., $z > 0$, all three determinants D_1, D_2 and D_3, defined in Eqs. (6.2) and (6.3), have to be negative: $D_a < 0$, $a = 1, 2, 3$. Given the half-life T_1 and the NMEs M_i and Λ_i, these three conditions are satisfied if each of the two half-lives T_2 and T_3 lies in specific intervals[6]:

$$\text{A)} \quad \begin{cases} \frac{\Lambda_1^2}{\Lambda_2^2}\frac{G_1}{G_2} T_1 < T_2 \le \frac{M_1\Lambda_1}{M_2\Lambda_2}\frac{G_1}{G_2} T_1, \\ \frac{(M_2^2\Lambda_1^2 - M_1^2\Lambda_2^2)\frac{G_2}{G_3}T_2}{(M_3^2\Lambda_1^2 - M_1^2\Lambda_3^2) + \frac{T_2 G_2}{T_1 G_1}(M_2^2\Lambda_3^2 - M_3^2\Lambda_2^2)} < T_3 < \frac{(M_2\Lambda_2\Lambda_1^2 - M_1\Lambda_1\Lambda_2^2)\frac{G_2}{G_3}T_2}{(M_3\Lambda_3\Lambda_1^2 - M_1\Lambda_1\Lambda_3^2) + \frac{T_2 G_2}{T_1 G_1}(M_2\Lambda_2\Lambda_3^2 - M_3\Lambda_3\Lambda_2^2)}; \end{cases}$$

$$\text{B)} \quad \begin{cases} \frac{M_1\Lambda_1}{M_2\Lambda_2}\frac{G_1}{G_2} T_1 < T_2 < \frac{M_1^2}{M_2^2}\frac{G_1}{G_2} T_1, \\ \frac{(M_2^2\Lambda_1^2 - M_1^2\Lambda_2^2)\frac{G_2}{G_3}T_2}{(M_3^2\Lambda_1^2 - M_1^2\Lambda_3^2) + \frac{T_2 G_2}{T_1 G_1}(M_2^2\Lambda_3^2 - M_3^2\Lambda_2^2)} < T_3 < \frac{(M_2\Lambda_2 M_1^2 - M_1\Lambda_1 M_2^2)\frac{G_2}{G_3}T_2}{(M_3\Lambda_3 M_1^2 - M_1\Lambda_1 M_3^2) + \frac{T_2 G_2}{T_1 G_1}(M_2\Lambda_2 M_3^2 - M_3\Lambda_3 M_2^2)} \end{cases}. \tag{6.7}$$

For the NMEs calculated with the CD-Bonn potential, the large basis and $g_A = 1.25$ and given $T_1 \neq 0$, the conditions for constructive interference, $z > 0$, read:

$$z > 0: \begin{cases} 0.14 T_1 < T_2 \le 0.16 T_1, & \frac{4.44 T_1 T_2}{3.74 T_1 - 0.93 T_2} \le T_3 \le \frac{2.10 T_1 T_2}{1.78 T_1 - 0.47 T_2}; \\ 0.16 T_1 < T_2 < 0.18 T_1, & \frac{4.44 T_1 T_2}{3.74 T_1 - 0.93 T_2} \le T_3 \le \frac{4.10 T_1 T_2}{3.44 T_1 - 0.81 T_2}. \end{cases} \tag{6.8}$$

[6]The quoted solutions are valid, as can be shown, provided $M_3/\Lambda_3 < M_2/\Lambda_2 < 0.5(1 + \sqrt{5}) M_3/\Lambda_3$, which is fulfilled for the NMEs given in Table I.

These conditions imply that given T_1, a constructive interference is possible only if T_2 lies in a relatively narrow interval and T_3 has a value in extremely narrow intervals, the interval for T_2 being determined by the value of T_1, while that for T_3—by T_1 and the interval for T_2. The fact that both the intervals for T_2 and T_3 are so narrow is a consequence of the values of the NMEs used, more precisely, of the fact that, for each of the two mechanisms discussed, the NMEs for the three nuclei considered differ by relatively little: we have $|M_i - M_j| \ll M_i,\ M_j$, $|\Lambda_i - \Lambda_j| \ll \Lambda_i,\ \Lambda_j$, $i \neq j = 1,\ 2,\ 3$, and typically $|M_i - M_j|/(0.5(M_i + M_j)) \sim 10^{-1}$, $|\Lambda_i - \Lambda_j|/(0.5(\Lambda_i + \Lambda_j)) \sim (10^{-2}\text{–}10^{-1})$. We get similar results for the other sets of NMEs, quoted in Table I and calculated with the large basis. In order to have a constructive interference in a much wider interval of values of T_2, i.e., to have the minimal value of T_2 much smaller than the maximal value of T_2 in case A) in Eq. (6.7), for instance, the following inequality has to be satisfied: $\Lambda_1/\Lambda_2 \ll M_1/M_2$. An inspection of Table I shows that this inequality is not satisfied by any of the relevant sets of NMEs. Numerically, the intervals of values of T_2 and T_3 given in Eq. (6.8), for which $z > 0$, are very similar to those quoted in Eq. (5.4).

For the value of $\mathrm{T}(^{76}\mathrm{Ge}) = 2.23 \times 10^{25}$ y, for instance, the conditions for a constructive interference are given by:

$$\begin{aligned} &3.18 \times 10^{24}\ \mathrm{y} < T_2 \leq 3.55 \times 10^{24}\ \mathrm{y}, \qquad \frac{1.19 T_2}{1.00\text{–}1.12 \times 10^{-26}\ \mathrm{y}^{-1} T_2} < T_3 < \frac{1.19 T_2}{1.00\text{–}1.18 \times 10^{-26}\ \mathrm{y}^{-1} T_2}, \\ &3.55 \times 10^{24}\ \mathrm{y} < T_2 < 3.97 \times 10^{24}\ \mathrm{y}, \qquad \frac{1.186 T_2}{1.00\text{–}1.117 \times 10^{-26}\ \mathrm{y}^{-1} T_2} < T_3 < \frac{1.189 T_2}{1.00\text{–}1.059 \times 10^{-26}\ \mathrm{y}^{-1} T_2}. \end{aligned} \tag{6.9}$$

Given the fact that $3.18 \times 10^{24}\ \mathrm{y} < T_2 \leq 3.97 \times 10^{24}$ y and that T_2 enters in the denominators of the limiting values of T_3 multiplied by $10^{-26}\ \mathrm{y}^{-1}$, the interval of values of T_3 of interest is extremely narrow. We have $z > 0$ for, e.g., $\mathrm{T}(^{76}\mathrm{Ge}) = 2.23 \times 10^{25}$ y, $\mathrm{T}(^{100}\mathrm{Mo}) = 3.7 \times 10^{24}$ y and $\mathrm{T}(^{130}\mathrm{Te}) = 4.58 \times 10^{24}$ y, as is also illustrated in Fig. 13.

There are cases in which one has $|\eta_\nu|^2 = 0$ or $|\eta_{\lambda'}|^2 = 0$. The general conditions for having $|\eta_\nu|^2 = 0$ or $|\eta_{\lambda'}|^2 = 0$ can be derived from Eqs. (6.1), (6.2), and (6.3) and read:

$$\begin{aligned} &|\eta_\nu|^2 = 0, |\eta_{\lambda'}|^2 \neq 0, \qquad \begin{cases} T_2 = \frac{\Lambda_1^2}{\Lambda_2^2} \frac{G_1}{G_2} T_1 \\ T_3 = \frac{(M_2 \Lambda_2 \Lambda_1^2 - M_1 \Lambda_1 \Lambda_2^2)\frac{G_2}{G_3} T_2}{(M_3 \Lambda_3 \Lambda_1^2 - M_1 \Lambda_1 \Lambda_3^2) + \frac{T_2 G_2}{T_1 G_1}(M_2 \Lambda_2 \Lambda_3^2 - M_3 \Lambda_3 \Lambda_2^2)}; \end{cases} \\ &|\eta_{\lambda'}|^2 = 0, |\eta_\nu|^2 \neq 0 \qquad \begin{cases} T_2 = \frac{M_1^2}{M_2^2} \frac{G_1}{G_2} T_1, \\ T_3 = \frac{(M_2 \Lambda_2 M_1^2 - M_1 \Lambda_1 M_2^2)\frac{G_2}{G_3} T_2}{(M_3 \Lambda_3 M_1^2 - M_1 \Lambda_1 M_3^2) + \frac{T_2 G_2}{T_1 G_1}(M_2 \Lambda_2 M_3^2 - M_3 \Lambda_3 M_2^2)}. \end{cases} \end{aligned} \tag{6.10}$$

They correspond to some of the limiting values of T_2 and T_3 in Eq. (6.7). We will illustrate them below numerically using the NMEs calculated with the CD-Bonn potential, the large basis and $g_A = 1.25$. If, for instance, one fixes $T_1 \equiv \mathrm{T}(^{76}\mathrm{Ge}) = 2.23 \times 10^{25}$, we have (i) $|\eta_\nu|^2 = 0$ (and zero interference term) for $T_2 = 3.18 \times 10^{24}$ y and $T_3 = 3.91 \times 10^{24}$ y; (ii) $|\eta_{\lambda'}|^2 = 0$ (and zero interference term) for $T_2 = 3.97 \times 10^{24}$ y and $T_3 = 4.93 \times 10^{24}$ y, where T_2 and T_3 denote the half-lives of ^{100}Mo and ^{130}Te, respectively. In general, given T_1 we have $|\eta_\nu|^2 = 0$, $|\eta_{\lambda'}|^2 \neq 0$ if

$$T_2 = 0.14 T_1, \qquad T_3 = \frac{2.10 T_1 T_2}{1.78 T_1 - 0.47 T_2} \cong 0.18 T_1, \tag{6.11}$$

and $|\eta_{\lambda'}|^2 = 0$, $|\eta_\nu|^2 \neq 0$ provided

$$T_2 = 0.18 T_1, \qquad T_3 = \frac{4.10 T_1 T_2}{3.44 T_1 - 0.81 T_2} \cong 0.22 T_1. \tag{6.12}$$

The conditions for having zero inteference term, $z = 0$, but $|\eta_\nu|^2 \neq 0$ or $|\eta_{\lambda'}|^2 \neq 0$, read:

$$\begin{cases} \frac{\Lambda_1^2}{\Lambda_2^2} \frac{G_1}{G_2} T_1 < T_2 < \frac{M_1^2}{M_2^2} \frac{G_1}{G_2} T_1, \\ T_3 = \frac{(M_2^2 \Lambda_1^2 - M_1^2 \Lambda_2^2)\frac{G_2}{G_3} T_2}{(M_3^2 \Lambda_1^2 - M_1^2 \Lambda_3^2) + \frac{T_2 G_2}{T_1 G_1}(M_2^2 \Lambda_3^2 - M_3^2 \Lambda_2^2)}. \end{cases} \tag{6.13}$$

Given T_1, the general conditions for destructive interference, i.e., for $z < 0$, can be derived in a similar way. They read:

$$\text{A)}\quad \begin{cases} 0 < T_2 \leq \frac{\Lambda_1^2}{\Lambda_2^2}\frac{G_1}{G_2}T_1, \\ 0 < T_3 < \frac{(M_2\Lambda_2\Lambda_1^2 - M_1\Lambda_1\Lambda_1^2)\frac{G_2}{G_3}T_2}{(M_3\Lambda_3\Lambda_1^2 - M_1\Lambda_1\Lambda_1^2) + \frac{T_2G_2}{T_1G_1}(M_2\Lambda_2\Lambda_3^2 - M_3\Lambda_3\Lambda_2^2)}; \end{cases} \tag{6.14}$$

$$\text{B)}\quad \begin{cases} \frac{\Lambda_1^2}{\Lambda_2^2}\frac{G_1}{G_2}T_1 < T_2 \leq \frac{M_1^2}{M_2^2}\frac{G_1}{G_2}T_1, \\ 0 < T_3 < \frac{(M_2^2\Lambda_1^2 - M_1^2\Lambda_2^2)\frac{G_2}{G_3}T_2}{(M_3^2\Lambda_1^2 - M_1^2\Lambda_3^2) + \frac{T_2G_2}{T_1G_1}(M_2^2\Lambda_3^2 - M_3^2\Lambda_2^2)}; \end{cases} \tag{6.15}$$

$$\text{C)}\quad \begin{cases} \frac{M_1^2}{M_2^2}\frac{G_1}{G_2}T_1 < T_2 < \frac{M_1\Lambda_1M_3 - \Lambda_3M_1^2}{M_2\Lambda_2M_3 - \Lambda_3M_2^2}\frac{G_1}{G_2}T_1, \\ 0 < T_3 < \frac{(M_2\Lambda_2M_1^2 - M_1\Lambda_1M_2^2)\frac{G_2}{G_3}T_2}{(M_3\Lambda_3M_1^2 - M_1\Lambda_1M_3^2) + \frac{T_2G_2}{T_1G_1}(M_2\Lambda_2M_3^2 - M_3\Lambda_3M_2^2)}; \end{cases} \tag{6.16}$$

$$\text{D)}\quad \begin{cases} T_2 \geq \frac{M_1\Lambda_1M_3 - \Lambda_3M_1^2}{M_2\Lambda_2M_3 - \Lambda_3M_2^2}\frac{G_1}{G_2}T_1. \\ T_3 > 0. \end{cases} \tag{6.17}$$

Obviously, one has to take into account the existing experimental lower limits on T_2 and T_3 in Eqs. (6.14), (6.15), (6.16), and (6.17). We will give next the "numerical" equivalent of the conditions (6.14), (6.15), (6.16), and (6.17), obtained with NMEs calculated with the CD-Bonn potential, the large basis and $g_A = 1.25$:

$$z < 0\text{:}\quad \begin{cases} T_2 \leq 0.14T_1, & T_3 \leq \frac{2.10T_1T_2}{1.78T_1 - 0.47T_2}; \\ 0.14T_1 < T_2 \leq 0.18T_1, & T_3 \leq \frac{4.44T_1T_2}{3.74T_1 - 0.93T_2}; \\ 0.18T_1 < T_2 < 4.23T_1, & T_3 \leq \frac{4.10T_1T_2}{3.44T_1 - 0.81T_2}; \\ T_2 \geq 4.23T_1, & T_3 > 0. \end{cases} \tag{6.18}$$

The intervals of values of T_2 and T_3 in Eqs. (6.14), (6.15), (6.16), (6.17), and (6.18) are very different from those corresponding to the case of two "noninterfering" $(\beta\beta)_{0\nu}$-decay mechanisms given in Eq. (5.4), the only exception being the second set of intervals in Eq. (6.18), which partially overlap with those in Eq. (5.4). This difference can allow us to discriminate experimentally between the two possibilities of $(\beta\beta)_{0\nu}$ decay being triggered by two "noninterfering" mechanisms or by two "destructively interfering" mechanisms. We have checked how the intervals of values of the half-life T_3 given in Table III, corresponding to NMEs derived with the CD-Bonn potential, $g_A = 1.25$ and the large basis, change when one uses the NMEs obtained with the same potential and basis, but using $g_A = 1.0$, as well as the NMEs found with the Argonne potential for $g_A = 1.25$, 1.0 and the large basis. The results are shown in Tables IV, V, and VI. We see that for certain values of the hypothetical half-lives of the two nuclei, the interval of allowed values of the half-life of the third nucleus becomes noticeably larger when calculated with NMEs, corresponding to $g_A = 1.0$ or to the Argonne potential. This is due to a relatively deep compensation between the three terms in the $(\beta\beta)_{0\nu}$-decay rate of the third nucleus in the case of a negative interference term (destructive interference).

TABLE IV. CD-Bonn potential and $g_A = 1$.

$T_{1/2}^{0\nu}$ [y] (fixed)	$T_{1/2}^{0\nu}$ [y] (fixed)	Allowed
$T(\text{Ge}) = 2.23 \times 10^{25}$	$T(\text{Mo}) = 5.8 \times 10^{24}$	$3 \times 10^{24} \leq T(\text{Te}) \leq 8.62 \times 10^{24}$
$T(\text{Ge}) = 2.23 \times 10^{25}$	$T(\text{Te}) = 3 \times 10^{24}$	$2.55 \times 10^{24} \leq T(\text{Mo}) \leq 6.18 \times 10^{24}$
$T(\text{Ge}) = 2.23 \times 10^{25}$	$T(\text{Te}) = 3 \times 10^{25}$	$1.33 \times 10^{25} \leq T(\text{Mo}) \leq 3.88 \times 10^{26}$
$T(\text{Ge}) = 10^{26}$	$T(\text{Mo}) = 5.8 \times 10^{24}$	$3.62 \times 10^{24} \leq T(\text{Te}) \leq 6.04 \times 10^{24}$
$T(\text{Ge}) = 10^{26}$	$T(\text{Te}) = 3 \times 10^{24}$	$3.11 \times 10^{24} \leq T(\text{Mo}) \leq 4.70 \times 10^{24}$
$T(\text{Ge}) = 10^{26}$	$T(\text{Te}) = 3 \times 10^{25}$	$2.15 \times 10^{25} \leq T(\text{Mo}) \leq 8.29 \times 10^{25}$

TABLE V. Argonne potential and $g_A = 1.25$.

$T_{1/2}^{0\nu}$ [y] (fixed)	$T_{1/2}^{0\nu}$ [y] (fixed)	Allowed
$T(\text{Ge}) = 2.23 \times 10^{25}$	$T(\text{Mo}) = 5.8 \times 10^{24}$	$3 \times 10^{24} \leq T(\text{Te}) \leq 9.22 \times 10^{24}$
$T(\text{Ge}) = 2.23 \times 10^{25}$	$T(\text{Te}) = 3 \times 10^{24}$	$2.55 \times 10^{24} \leq T(\text{Mo}) \leq 7.92 \times 10^{24}$
$T(\text{Ge}) = 2.23 \times 10^{25}$	$T(\text{Te}) = 3 \times 10^{25}$	$1.19 \times 10^{25} \leq T(\text{Mo}) \leq 2.55 \times 10^{27}$
$T(\text{Ge}) = 10^{26}$	$T(\text{Mo}) = 5.8 \times 10^{24}$	$3.15 \times 10^{24} \leq T(\text{Te}) \leq 5.85 \times 10^{24}$
$T(\text{Ge}) = 10^{26}$	$T(\text{Te}) = 3 \times 10^{24}$	$3.25 \times 10^{24} \leq T(\text{Mo}) \leq 5.49 \times 10^{24}$
$T(\text{Ge}) = 10^{26}$	$T(\text{Te}) = 3 \times 10^{25}$	$2.08 \times 10^{25} \leq T(\text{Mo}) \leq 1.20 \times 10^{26}$

TABLE VI. Argonne Potential and $g_A = 1$.

$T^{0\nu}_{1/2}$ [y] (fixed)	$T^{0\nu}_{1/2}$ [y] (fixed)	Allowed
$T(\mathrm{Ge}) = 2.23 \times 10^{25}$	$T(\mathrm{Mo}) = 5.8 \times 10^{24}$	$3 \times 10^{24} \leq T(\mathrm{Te}) \leq 1.11 \times 10^{25}$
$T(\mathrm{Ge}) = 2.23 \times 10^{25}$	$T(\mathrm{Te}) = 3 \times 10^{24}$	$2.63 \times 10^{24} \leq T(\mathrm{Mo}) \leq 2.04 \times 10^{25}$
$T(\mathrm{Ge}) = 2.23 \times 10^{25}$	$T(\mathrm{Te}) = 3 \times 10^{25}$	$9.19 \times 10^{24} \leq T(\mathrm{Mo}) \leq 2.36 \times 10^{26}$
$T(\mathrm{Ge}) = 10^{26}$	$T(\mathrm{Mo}) = 5.8 \times 10^{24}$	$3 \times 10^{24} \leq T(\mathrm{Te}) \leq 5.07 \times 10^{24}$
$T(\mathrm{Ge}) = 10^{26}$	$T(\mathrm{Te}) = 3 \times 10^{24}$	$3.82 \times 10^{24} \leq T(\mathrm{Mo}) \leq 9.44 \times 10^{24}$
$T(\mathrm{Ge}) = 10^{26}$	$T(\mathrm{Te}) = 3 \times 10^{25}$	$1.96 \times 10^{25} \leq T(\mathrm{Mo}) \leq 6.54 \times 10^{26}$

Similar analysis can be performed for any other pair of interfering mechanisms assumed to be operative in $(\beta\beta)_{0\nu}$ decay. We note also that the extension of the analysis to more than two mechanisms generating the $(\beta\beta)_{0\nu}$ decay is rather straightforward.

Finally, we would like to point out one additional consequence of the positivity conditions and the condition the interference term should satisfy when two interfering mechanisms are responsible for the $(\beta\beta)_{0\nu}$ decay. Let us denote the two fundamental parameters characterizing the two mechanisms by η_β and η_κ. Then, given the half-life of one isotope, say of ^{76}Ge (T_1), and an experimental lower bound on the half-life of a second isotope, e.g., of ^{130}Te (T_3), the conditions $|\eta_\beta|^2 > 0$, $|\eta_\kappa|^2 > 0$ and $-|\eta_\beta||\eta_\kappa| \leq |\eta_\beta||\eta_\kappa|\cos\alpha_{\beta\kappa} \leq |\eta_\beta||\eta_\kappa|$, imply a constraint on the half-life of any third isotope, say of ^{100}Mo (T_2). This latter constraint depends noticeably on the type of the two interfering mechanisms generating the $(\beta\beta)_{0\nu}$ decay and can be used, in principle, to discriminate between the different possible pairs of interfering mechanisms. Below we illustrate this result by deriving the constraint one obtains on the half-life of ^{100}Mo, T_2, assuming that the half-life of ^{76}Ge is $T_1 = 2.23 \times 10^{25}$ y and taking into account the current experimental lower bound on the half-life of ^{130}Te, $T_3 > 3.0 \times 10^{24}$ y. Using these data as input, the NMEs calculated with the CD-Bonn and Argonne potentials, the large basis and $g_A = 1.25$, we get the following constraint on T_2 for the different pairs of interfering mechanisms discussed by us (the numbers in brackets are obtained with the NMEs corresponding to the Argonne potential, unless otherwise indicated).

Light Neutrino and gluino exchange mechanisms:

$$T_2 \equiv T^{0\nu}_{1/2}(^{100}\mathrm{Mo}) > 2.46(2.47) \times 10^{24}\ \mathrm{y}. \qquad (6.19)$$

Increasing the value of $T^{0\nu}_{1/2}(^{76}\mathrm{Ge})$ leads to the increasing of the value of the lower limit.

Light Neutrino and LH Heavy neutrino exchange mechanisms:

$$T^{0\nu}_{1/2}(^{100}\mathrm{Mo}) > 2.78(2.68) \times 10^{24}\ \mathrm{y}. \qquad (6.20)$$

The value of the lower limit increases with the increasing of the value of the half-life of ^{76}Ge.

LH Heavy neutrino and gluino exchange mechanisms:

$$1.36 \times 10^{24}\ \mathrm{y} < T^{0\nu}_{1/2}(^{100}\mathrm{Mo}) < 3.42 \times 10^{24}\ \mathrm{y}. \qquad (6.21)$$

Increasing the value of $T^{0\nu}_{1/2}(^{76}\mathrm{Ge})$ leads to a shift of the interval to larger values, and for a sufficiently large $T^{0\nu}_{1/2}(^{76}\mathrm{Ge}) > 10^{26}$ y—even just to a lower bound on $T^{0\nu}_{1/2}(^{100}\mathrm{Mo})$. For $T_1 = 10^{26}$ y, for instance, we find $4.19 \times 10^{24}\ \mathrm{y} < T^{0\nu}_{1/2}(^{100}\mathrm{Mo}) < 3.39 \times 10^{25}$ y.

Using the NMEs derived with the Argonne potential we find a very different result—only a lower bound: $T^{0\nu}_{1/2}(^{100}\mathrm{Mo}) > 5.97 \times 10^{23}$ y. The difference between the results obtained with the two sets of NMEs can be traced to the fact that the determinant D in Eqs. (6.1) and (6.2), calculated with the second set of NMEs, has the opposite sign to that calculated with the first set of NMEs. As a consequence, the dependence of the physical solutions for $|\eta^L_N|^2$ and $|\eta_{\lambda'}|^2$ on T_1, T_2 and T_3 in the two cases of NMEs is very different.

Squarks-neutrino and gluino exchange mechanisms:

$$T^{0\nu}_{1/2}(^{100}\mathrm{Mo}) > 7.92(22.1) \times 10^{23}\ \mathrm{y}. \qquad (6.22)$$

For larger values of $T^{0\nu}_{1/2}(^{76}\mathrm{Ge})$, this lower bound assumes larger values.

We see that the two sets of NMEs lead to quite different results in the cases of the LH heavy neutrino and gluino exchange and squarks-neutrino and gluino exchange mechanisms. Nevertheless, the constraints thus obtained can be used, e.g., to exclude some of the possible cases of two interfering mechanisms inducing the $(\beta\beta)_{0\nu}$ decay. Indeed, if, for instance, it is confirmed that $T^{0\nu}_{1/2}(^{76}\mathrm{Ge}) = 2.23 \times 10^{25}$ y, and in addition it is established, taking all relevant uncertainties into account, that $T^{0\nu}_{1/2}(^{100}\mathrm{Mo}) \leq 10^{24}$ y, that combined with the experimental lower limit on $T^{0\nu}_{1/2}(^{130}\mathrm{Te})$ would rule out (i) the light neutrino and gluino exchanges, and (ii) the light neutrino and LH heavy neutrino exchanges, as possible mechanisms generating the $(\beta\beta)_{0\nu}$ decay.

VII. SUMMARY AND CONCLUSIONS

In the present article we have considered the possibility of several different mechanisms contributing to the $(\beta\beta)_{0\nu}$-decay amplitude in the general case of CP nonconservation. The mechanisms discussed are light Majorana neutrino exchange, exchange of heavy Majorana neutrinos coupled to $(V - A)$ currents, exchange of heavy Majorana neutrinos coupled to $(V + A)$ currents,

lepton charge nonconserving couplings in SUSY theories with R-parity breaking. Of the latter we have concentrated on the so-called ''dominant gluino exchange'' mechanism. Each of these mechanisms is characterized by a specific fundamental lepton number violating parameter. The latter are defined in Sec. II. We have investigated in detail the cases of two ''noninterfering'' and two interfering mechanisms, generating the $(\beta\beta)_{0\nu}$ decay. In the analysis we have performed, we have used hypothetical $(\beta\beta)_{0\nu}$-decay half-lives of the following three isotopes: ^{76}Ge, ^{100}Mo and ^{130}Te. They are denoted as T_1, T_2 and T_3, respectively. Four sets of nuclear matrix elements of the decays of these three nuclei were utilised: they were obtained with two different nucleon-nucleon potentials (CD-Bonn and Argonne) and two different values of the axial-coupling constant $g_A = 1.25, 1.0$ (see Table I).

If the $(\beta\beta)_{0\nu}$ decay is induced by two ''noninterfering'' mechanisms, which for concreteness we have considered to be the light LH Majorana neutrino exchange and the heavy RH Majorana neutrino exchange with $(V + A)$ currents, one can determine the squares of the absolute values of the two LNV parameters, characterising these mechanisms, $|\eta_\nu|^2$ and $|\eta_R|^2$, from data on the half-lives of two nuclear isotopes. We have done that using as input all three possible pairs of half-lives of ^{76}Ge, ^{100}Mo and ^{130}Te, chosen from the intervals given in Eq. (4.3) and satisfying the existing experimental lower limits, as well as the half-life of the $(\beta\beta)_{0\nu}$ decay of ^{76}Ge, claimed to be observed in [12]: $T^{0\nu}_{1/2}(^{76}\mathrm{Ge}) = 2.23^{+0.44}_{-0.31} \times 10^{25}$ y. We find that if the half-life of one of the three nuclei is measured, the requirement that $|\eta_\nu|^2 \geq 0$ and $|\eta_R|^2 \geq 0$ (positivity condition) constrains the other two half-lives (and the $(\beta\beta)_{0\nu}$-decay half-life of any other $(\beta\beta)_{0\nu}$-decaying isotope for that matter) to lie in specific intervals, determined by the measured half-life and the relevant NMEs (see Eqs. (5.3), (5.4), (5.5), and (5.6)). This feature is common to all cases of two ''noninterfering'' mechanisms generating the $(\beta\beta)_{0\nu}$ decay. The indicated specific half-life intervals for the various isotopes, are stable with respect to the change of the NMEs (within the sets of NMEs considered by us) used to derive them. The intervals depend, in general, on the type of the two ''noninterfering'' mechanisms. However, these differences in the cases of the $(\beta\beta)_{0\nu}$ decay triggered by the exchange of heavy Majorana neutrinos coupled to $(V + A)$ currents and i) the light Majorana neutrino exchange, or ii) the gluino exchange mechanism, or iii) the squark-neutrino exchange mechanism, are extremely small. One of the consequences of this feature of the different pairs of ''noninterfering'' mechanisms considered by us is that if it will be possible to rule out one of them as the cause of $(\beta\beta)_{0\nu}$ decay, most likely one will be able to rule out all three of them. Using the indicated difference to get information about the specific pair of ''noninterfering'' mechanisms possibly operative in $(\beta\beta)_{0\nu}$ decay requires, in the cases considered by us, an extremely high precision in the measurement of the $(\beta\beta)_{0\nu}$-decay half-lives of the isotopes considered. The levels of precision required seem impossible to achieve in the foreseeable future. If it is experimentally established that any of the indicated intervals of half-lives lies outside the interval of physical solutions of $|\eta_\nu|^2$ and $|\eta_R|^2$, obtained taking into account all relevant uncertainties, one would be led to conclude that the $(\beta\beta)_{0\nu}$ decay is not generated by the two mechanisms considered. The constraints under discussion will not be valid, in general, if the $(\beta\beta)_{0\nu}$ decay is triggered by two interfering mechanisms with a non-negligible (destructive) interference term, or by more than two mechanisms none of which plays a subdominat role in $(\beta\beta)_{0\nu}$ decay.

We have studied also the dependence of the physical solutions for $|\eta_\nu|^2$ and $|\eta_R|^2$ obtained on the NMEs used. Some of the results of this study are presented graphically in Figs. 8 and 9. We found that the solutions can exhibit a significant variation with the NMEs used. Given the half-life T_1, the interval of allowed values of the half-life of the second nucleus T_2, determined from the positivity conditions, $|\eta_\nu|^2 \geq 0$, $|\eta_R|^2 \geq 0$, changes somewhat with the change of the NMEs. The solution values of the parameters $|\eta_\nu|^2$ and $|\eta_R|^2$, obtained with the two different sets of the NMEs, can differ drastically in the vicinity of the maximum and minimum values of T_2 (Figs. 8 and 9). If a given extreme value of T_2, say $\max(T_2)$, obtained with one set of NMEs, belongs to the interval of allowed values of T_2, found with a second set of NMEs, one of the fundamental parameters, calculated at $\max(T_2)$ with the first set of NMEs can be zero, and can have a relatively large nonzero value when calculated with the second set of NMEs. Moreover, there are narrow intervals of values of T_2 for which there exist physical solutions for $|\eta_\nu|^2$ and $|\eta_R|^2$ if one uses the NMEs obtained with the CD-Bonn potential and there are no physical solutions for the NMEs derived with the Argonne potential. If the measured value of T_2 falls in such an interval, this can imply that either the two mechanisms considered are not at work in $(\beta\beta)_{0\nu}$ decay, or one of the two sets of NMEs does not describe correctly the nuclear transitions.

Neutrinoless double beta decay can be generated by two competitive mechanisms whose interference contribution to the $(\beta\beta)_{0\nu}$-decay rates is non-negligible. In the case when two interfering mechanisms are responsible for the $(\beta\beta)_{0\nu}$ decay, the squares of the absolute values of the two relevant parameters and the interference term parameter, which involves the cosine of an unknown relative phase of the two fundamental parameters, can be uniquely determined, in principle, from data on the half-lives of three nuclei. We have analyzed in detail the case of light Majorana neutrino exchange and gluino exchange. In this case the parameters which are determined from data on the half-lives are $|\eta_\nu|^2$, $|\eta_{\lambda'}|^2$ and $z = 2\cos\alpha|\eta_\nu||\eta_{\lambda'}|$. The physical solutions for these parameters have to satisfy

the conditions $|\eta_\nu|^2 \geq 0$, $|\eta_{\lambda'}|^2 \geq 0$ and $-2|\eta_\nu||\eta_{\lambda'}| \leq z \leq 2|\eta_\nu||\eta_{\lambda'}|$. The latter condition implies that given the half-lives of two isotopes, T_1 and T_2, the half-life of any third isotope T_3 is constrained to lie is a specific interval, if the mechanisms considered are indeed generating the $(\beta\beta)_{0\nu}$ decay. If further the half-life of one isotope T_1 is known, for the interference to be constructive (destructive) the half-lives of any other pair of isotopes T_2 and T_3, should belong to specific intervals. These intervals depend on whether the interference between the two contributions in the $(\beta\beta)_{0\nu}$-decay rate is constructive or destructive. We have derived in analytic form the general conditions for (i) constructive interference ($z > 0$), (ii) destructive interference ($z < 0$), (iii) $|\eta_\nu|^2 = 0$, $|\eta_{\lambda'}|^2 \neq 0$, (iv) $|\eta_\nu|^2 \neq 0$, $|\eta_{\lambda'}|^2 = 0$ and (v) $z = 0$, $|\eta_\nu|^2 \neq 0$, $|\eta_{\lambda'}|^2 \neq 0$.

We have found that, given T_1, a constructive interference is possible only if T_2 lies in a relatively narrow interval and T_3 has a value in extremely narrow intervals, the interval for T_2 being determined by the value of T_1, while that for T_3—by T_1 and the interval for T_2. The fact that both the intervals for T_2 and T_3 are so narrow is a consequence of the fact that, for each of the two mechanisms discussed, the NMEs for the three nuclei considered differ relatively little: the relative difference between the nuclear matrix elements of any two nuclei does not exceed 10%.

The intervals of values of T_2 and T_3 corresponding to destructive interference (Eqs. (6.14), (6.15), (6.16), (6.17), and (6.18)) are very different from those corresponding to the cases of constructive interference and of the two ''noninterfering'' $(\beta\beta)_{0\nu}$-decay mechanisms we have considered (Eq. (5.4)). Within the set of $(\beta\beta)_{0\nu}$-decay mechanisms studied by us, this difference can allow to discriminate experimentally between the possibilities of the $(\beta\beta)_{0\nu}$ decay being triggered by two destructively interfering mechanisms or by two ''constructively interfering'' or by two ''noninterfering'' mechanisms.

We have shown also that further significant constraints on the physical solutions for the fundamental parameter $|\eta_\nu|^2$ in the case of the light Majorana neutrino exchange mechanism and the gluino exchange (or any other interfering) mechanism can be obtained by using the current and the prospective upper bounds on the absolute scale of neutrino masses from the past [44,45] and the upcoming KATRIN [45] ^3H β-decay experiments of 2.3 eV and 0.2 eV, respectively. Our results show that the KATRIN prospective upper bound of 0.2 eV, if reached, could imply particularly stringent constraints in the cases of destructively interfering mechanisms one of which is the light neutrino exchange, to the point of strongly disfavoring (or even excluding) some of them. The KATRIN prospective upper bound could be used to constrain also the fundamental parameters of two ''noninterfering'' mechanisms, one of which is the light Majorana neutrino exchange. This bound could eliminate, in particular, some parts of the half-life solution intervals where there is a significant dependence of the values of $|\eta_\nu|^2$ obtained on the set of NMEs used.

The measurements of the half-lives with rather high precision and the knowledge of the relevant nuclear matrix elements with relatively small uncertainties is crucial for establishing whether more than one mechanisms are operative in $(\beta\beta)_{0\nu}$ decay. The method considered by us can be generalized to the case of more than two $(\beta\beta)_{0\nu}$-decay mechanisms. It allows to treat the cases of CP conserving and CP nonconserving couplings generating the $(\beta\beta)_{0\nu}$ decay in a unique way.

ACKNOWLEDGMENTS

This work was supported in part by the INFN program on ''Astroparticle Physics'', by the Italian MIUR program on ''Neutrinos, Dark Matter and Dark Energy in the Era of LHC'' (A. M. and S. T. P.) and by the World Premier International Research Center Initiative (WPI Initiative), MEXT, Japan (S. T. P.). A. F. and F. Š. acknowledge support of the Deutsche Forschungsgemeinschaft within Project No. 436 SLK 17/298. The work of F. Š. was also partially supported by the VEGA Grant agency of the Slovak Republic under Contract No. 1/063/09.

Note Added.—The possibility of several mechanisms being operative in $(\beta\beta)_{0\nu}$ decay is also discussed in another recent preprint [48], where the sets of nuclear matrix elements given in Table I are also used. However, the aspects of the problem of multiple mechanisms generating the $(\beta\beta)_{0\nu}$ decay investigated in the present article and in the preprint [48] are very different and, apart from the description of the nuclear matrix elements, the two studies practically do not overlap.

[1] B. Pontecorvo, Zh. Eksp. Teor. Fiz. **33**, 549 (1957); [Sov. Phys. JETP**6**, 429 (1957)]; Zh. Eksp. Teor. Fiz. **34**, 247 (1958); [Sov. Phys. JETP **7**, 172 (1958).
[2] Z. Maki, M. Nakagawa, and S. Sakata, Prog. Theor. Phys. **28**, 870 (1962).
[3] B. Pontecorvo, Zh. Eksp. Teor. Fiz. **53**, 1717 (1967) [Sov. Phys. JETP **26**, 984 (1968)].
[4] S. M. Bilenky, S. Pascoli, and S. T. Petcov, Phys. Rev. D **64**, 053010 (2001).
[5] K. Nakamura *et al.* (Particle Data Group), J. Phys. G **37**, 075021 (2010).
[6] C. E. Aalseth *et al.*, Phys. At. Nucl. **63**, 1225 (2000).
[7] C. Arnaboldi *et al.* (CUORICINO Collaboration), Phys. Rev. C **78**, 035502 (2008).

[8] A. S. Barabash (NEMO Collaboration), J. Phys.: Conf. Ser. **173**, 012008 (2009).
[9] F. Šimkovic *et al.*, Phys. Rev. C **79**, 055501 (2009).
[10] H. V. Klapdor-Kleingrothaus *et al.*, Nucl. Phys. B, Proc. Suppl. **100**, 309 (2001).
[11] H. V. Klapdor-Kleingrothaus *et al.*, Mod. Phys. Lett. A **16**, 2409 (2001).
[12] H. V. Klapdor-Kleingrothaus *et al.*, Phys. Lett. B **586**, 198 (2004).
[13] F. Avignone, Nucl. Phys. B, Proc. Suppl. **143**, 233 (2005).
[14] S. Pascoli, S. T. Petcov, and L. Wolfenstein, Phys. Lett. B **524**, 319 (2002); S. Pascoli and S. T. Petcov, Phys. Lett. B **544**, 239 (2002); **580**, 280 (2004); Phys. Rev. D **77**, 113003 (2008); S. Pascoli, S. T. Petcov, and T. Schwetz, Nucl. Phys. **B734**, 24 (2006); see also, e.g., S. T. Petcov, Physica Scripta **T121**, 94 (2005).
[15] J. Schechter and J. W. F. Valle, Phys. Rev. D **25**, 2951 (1982); E. Takasugi, Phys. Lett. B **149**, 372 (1984).
[16] S. M. Bilenky and S. T. Petcov, Rev. Mod. Phys. **59**, 671 (1987).
[17] F. Šimkovic, J. D. Vergados, and A. Faessler, Phys. Rev. D **82**, 113015 (2010).
[18] F. Šimkovic, G. Pantis, J. D. Vergados, and A. Faessler, Phys. Rev. C **60**, 055502 (1999).
[19] V. A. Rodin, A. Faessler, F. Šimkovic, and P. Vogel, Phys. Rev. C **68**, 044302 (2003); Nucl. Phys. **A766**, 107 (2006); **A793**, 213(E) (2007).
[20] S. M. Bilenky, J. Hosek, and S. T. Petcov, Phys. Lett. B **94**, 495 (1980).
[21] J. Schechter and J. W. F. Valle, Phys. Rev. D **22**, 2227 (1980); M. Doi, T. Kotani, and E. Takasugi, Phys. Lett. B **102**, 323 (1981).
[22] F. Šimkovic, A. Faessler, V. A. Rodin, P. Vogel, and J. Engel, Phys. Rev. C **77**, 045503 (2008).
[23] A. Halprin, P. Minkowski, H. Promakoff, and S. P. Rosen, Phys. Rev. D **13**, 2567 (1976).
[24] S. Antusch, J. P. Baumann, and E. Fernandez-Martinez, Nucl. Phys. **B810**, 369 (2009); S. Antusch *et al.*, J. High Energy Phys. 10 (2006) 084.
[25] R. Mohapatra and G. Senjanovic, Phys. Rev. D **23**, 165 (1981); V. Tello *et al.*, Phys. Rev. Lett. **106**, 151801 (2011).
[26] Y. Zhang *et al.*, Nucl. Phys. **B802**, 247 (2008).
[27] A. Halprin, S. T. Petcov, and S. P. Rosen, Phys. Lett. B **125**, 335 (1983).
[28] R. Mohapathra, Phys. Rev. D **34**, 3457 (1986).
[29] J. D. Vergados, Phys. Lett. B **184**, 55 (1987).
[30] M. Hirsch, H. V. Klapdor-Kleingrothaus, and S. G. Kovalenko, Phys. Rev. Lett. **75**, 17 (1995); Phys. Rev. D **53**, 1329 (1996).
[31] A. Faessler, S. G. Kovalenko, F. Šimkovic, and J. Schwieger, Phys. Rev. Lett. **78**, 183 (1997); A. Faessler, S. G. Kovalenko, and F. Šimkovic, Phys. Rev. D **58**, 115004 (1998).
[32] A. Wodecki and W. A. Kamiński, Phys. Rev. C **59**, R1232 (1999); A. Wodecki, W. A. Kamiński, and F. Šimkovic, Phys. Rev. D **60**, 115007 (1999).
[33] G. Prézeau, M. Ramsey-Musolf, and P. Vogel, Phys. Rev. D **68**, 034016 (2003).
[34] A. Faessler, S. Kovalenko, and F. Šimkovic, Phys. Rev. D **58**, 055004 (1998).
[35] M. Hirsch and J. W. F. Valle, Nucl. Phys. **B557**, 60 (1999); M. Hirsch, J. C. Romao, and J. W. F. Valle, Phys. Lett. B **486**, 255 (2000).
[36] M. Hirsch, H. V. Klapdor-Kleingrothaus, and S. G. Kovalenko, Phys. Lett. B **372**, 181 (1996); **381**, 488(E) (1996).
[37] H. Päs, M. Hirsch, and H. V. Klapdor-Kleingrothaus, Phys. Lett. B **459**, 450 (1999).
[38] A. Faessler, Th. Gutsche, S. Kovalenko, and F. Šimkovic, Phys. Rev. D **77**, 113012 (2008).
[39] A. Faessler, S. Kovalenko, F. Šimkovic, and J. Schwieger, Phys. Rev. Lett. **78**, 183 (1997); Phys. At. Nucl. **61**, 1229 (1998).
[40] A. Faessler, S. Kovalenko, and F. Šimkovic, Phys. Rev. D **58**, 115004 (1998).
[41] D. S. Delion, J. Dukelsky, and P. Schuck, Phys. Rev. C **55**, 2340 (1997); F. Krmpotić *et al.*, Nucl. Phys. **A637**, 295 (1998).
[42] M. K. Cheoun, A. Bobyk, A. Faessler, F. Šimkovic, and G. Teneva, Nucl. Phys. **A561**, 74 (1993).
[43] F. Šimkovic, A. Faessler, H. Müther, V. Rodin, and M. Stauf, Phys. Rev. C **79**, 055501 (2009).
[44] V. Lobashev *et al.*, Nucl. Phys. **A719**, C153 (2003).
[45] K. Eitel *et al.*, Nucl. Phys. B, Proc. Suppl. **143**, 197 (2005).
[46] S. Pascoli, S. T. Petcov, and L. Wolfenstein, Phys. Lett. B **524**, 319 (2002).
[47] S. M. Bilenky and S. T. Petcov, arXiv:hep-ph/0405237.
[48] Amand Faessler, G. L. Fogli, E. Lisi, A. M. Rottuno, and F. Šimkovic, arXiv:1103.2504.